nature ecology & evolution

Article

https://doi.org/10.1038/s41559-025-02795-4

Enlargement of sternum traits facilitated the evolution of powered flight in birds

Received: 17 September 2024

Accepted: 11 June 2025

Published online: 24 July 2025

Check for updates

Talia M. Lowi-Merri[1,2,3] ✉, Roger Benson[4], Han Hu[5], Jingmai O'Connor[6], Santiago Claramunt[2,3] & David C. Evans[2,3]

An enlarged sternum with a prominent keel is a central feature of the flight apparatus of modern birds. However, sterna of near-bird dinosaurs (Pennaraptora) and early avialans are either substantially different from those of living birds or absent altogether, raising questions about how specialized sternal structures evolved in birds and how they are related to function. This remains poorly understood because of the fragmentary nature of the fossil record, and the challenges in inferring form and function from crushed fossils. We use ancestral character estimations to trace sternal trait acquisition through the bird stem group, and multivariate phylogenetic regressions to analyse relationships between sternum morphology, body mass and flight capabilities. We find that sternum evolution was episodic: basal members of Pennaraptora had proportionally small sterna, which became larger and more craniocaudally elongated in Avialae. This enlargement precedes the appearance of a midline ridge, a possible precursor of the sternal keel, in Pygostylia. Sternum size increased again in crownward Ornithuromorpha, alongside a fully formed sternal keel and enlarged caudal projections, both critical areas of flight muscle attachment. Sternal experimentation in relation to flight characteristics occurs several times throughout Pennaraptora, including within Paraves and Enantiornithes, indicating that powered flight may have evolved several times before proliferating in crown-group birds.

The evolution of powered flight was a key locomotor innovation that expanded the ecological potential of bird ancestors, leading to remarkable diversity among modern birds (Neornithes)[1,2]. An enlarged sternum with a prominent keel is a key feature of the powered flight apparatus, providing an increased area for the attachment of the two crucial flight muscles (m. pectoralis and m. supracoracoideus) and allowing for greater power to be generated by the flight stroke[3–5]. Selective pressures associated with the evolution of flight have shaped the morphology of the sternum[6], and the appearance of a large, keeled sternum in fossil species is one of several morphological novelties that facilitated the evolution of neornithine-like flight along the bird stem lineage[3–5,7–17]. However, the evolution of sternum morphology in stem birds has not been quantitatively analysed, leaving gaps in our understanding of avian flight origins. Here, neornithine powered flight is considered to be sternum-anchored, because the flight muscles attach onto an enlarged, keeled sternum, which facilitates stronger flight capabilities.

Pennaraptoran stem birds—including dromaeosaurid dinosaurs such as *Microraptor* and early avialans *Archaeopteryx* and

[1]Department of Anatomy, New York Institute of Technology, College of Osteopathic Medicine, Old Westbury, NY, USA. [2]Department of Ecology and Evolutionary Biology, University of Toronto, Toronto, Ontario, Canada. [3]Department of Natural History, Royal Ontario Museum, Toronto, Ontario, Canada. [4]Division of Paleontology, American Museum of Natural History, New York, NY, USA. [5]Key Laboratory of Vertebrate Evolution and Human Origins, Institute of Vertebrate Paleontology and Paleoanthropology, Chinese Academy of Sciences, Beijing, China. [6]Negaunee Integrative Research Center, Field Museum of Natural History, Chicago, IL, USA. ✉e-mail: talialowimerri@gmail.com

https://doi.org/10.1038/s41559-025-02795-4

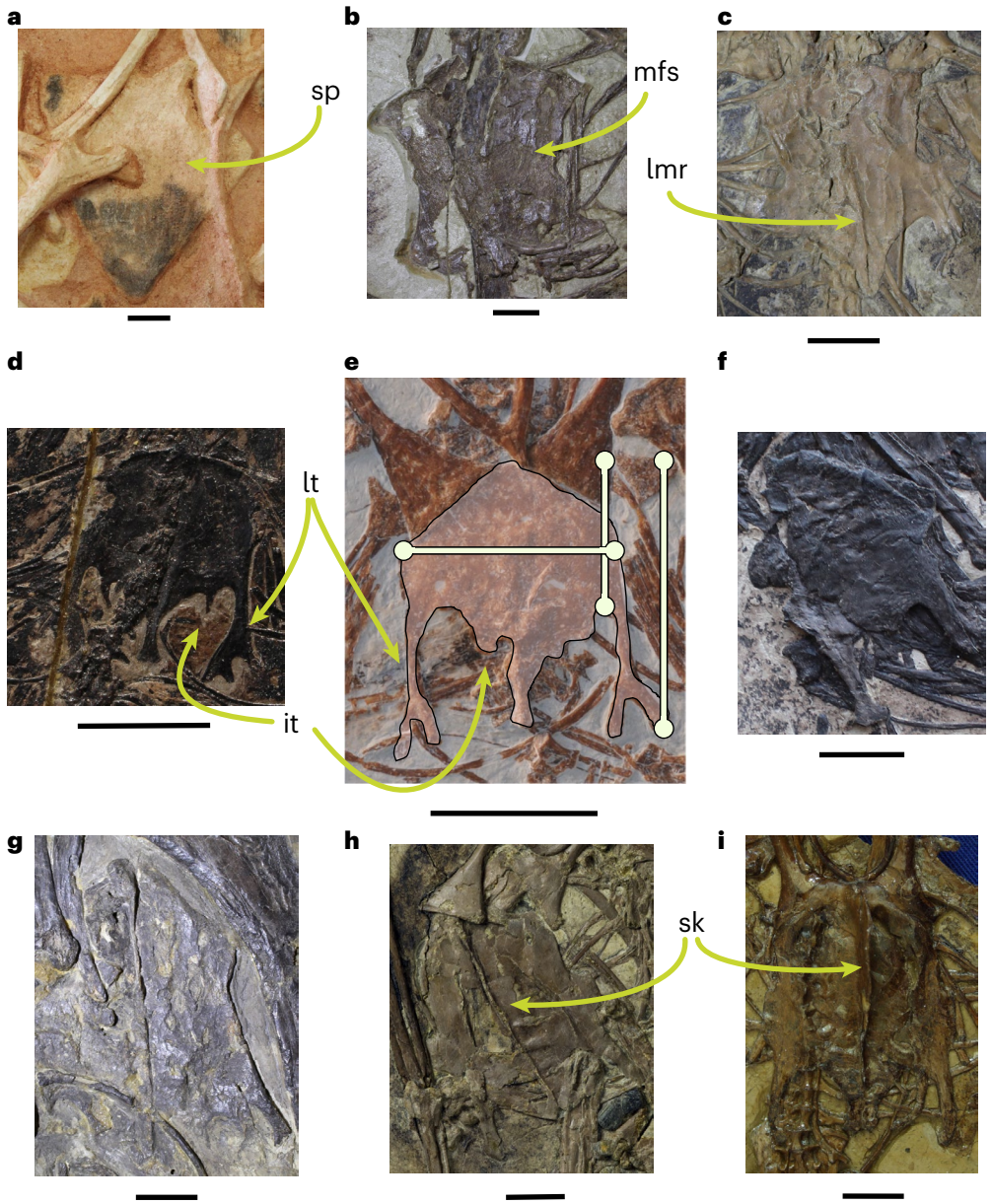

Fig. 1 | Fossil sterna from representative taxa included in the study. a, *Khaan mckennai* (Pennaraptora: Oviraptorosauria). **b**, *Microraptor gui* (Paraves: Dromaeosauridae). **c**, *Confuciusornis sanctus* (Avialae: Confuciusornithidae). **d**, *Longirostravis hani* (Ornithothoraces: Enantiornithes). **e**, *Rapaxavis pani* (Ornithothoraces: Enantiornithes) (showing measurements included in analyses: footprint area, width, minimum length, maximum length). **f**, *Fortunguavis xiaotaizicus* (Ornithothoraces: Enantiornithes). **g**, *Archaeorhynchus spathula* (Ornithothoraces: Ornithuromorpha). **h**, *Iteravis huchzermeyeri* (Ornithothoraces: Ornithuromorpha). **i**, *Gansus yumenensis* (Ornithothoraces: Ornithuromorpha). Abbreviations: it, intermediate trabeculae; lmr, low midline ridge; lt, lateral trabeculae; mfs, medially fused sternum; sk, sternal keel; sp, sternal plate (unfused). Scale bars, 10 mm.

Confuciusornis—show a combination of dinosaur- and bird-like features, both in the sternum (Fig. 1) and in the entire skeleton[18]. While wing and feather traits have been analysed extensively to study flight evolution[19–28], the details of how and when powered flight originated remain contentious. A few flight origin hypotheses dominate the literature, many of which conflict with one another[7,21,28–31]. Importantly, an ossified sternum is absent from several key transitional taxa with wing-like feather arrays, including *Archaeopteryx*, *Sapeornis* and *Anchiornis*[32–34]. Other stem birds preserve sterna that are smaller than in living birds, unfused or lacking a keel, such as in *Jeholornis*[35], *Confuciusornis*[36] and various enantiornithines[37–39]. Most research on flight origins has focused on wing functional morphology and biomechanics[19–25], and has only recently examined other crucial elements of the flight apparatus, such as the pectoral girdle[40–42], containing the shoulder elements and sternum. Comparative analysis of sternum morphometrics in living birds provides evidence that two main sternal features are associated with the presence of powered flight, and may be used to infer flight ability in fossil birds, at least within the crown group: (1) a large sternum relative to body size and (2) the presence of a deep and/or cranially projected sternal keel[6,43]. However, sternal morphology varies widely among stem birds in ways that contrast with modern bird sterna, despite several fossil pennaraptoran taxa being suggested to have been capable of some form of powered flight. Among the closest dinosaur relatives of avialans, the dromaeosaurid *Microraptor* has a small, rectangular sternum that is fused along the midline, modified from the unfused pair of sternal plates in more basal maniraptoran dinosaurs, and lacks any clear evidence of a keel[44,45]. The sternum in *Confuciusornis* from the more derived avialan clade

Pygostylia is also medially fused, with some specimens showing a slight ridge along the midline, having been interpreted as a keel homologue, vestige of a broken keel or the base of a larger cartilaginous keel[5,46,47]. Further crownward, Enantiornithes exhibits a wide variety of derived sternal morphologies, including keel-like structures of varied depths and differing arrangements of lateral and intermediate trabeculae or bony projections[12,48–51]. The keel is fully formed in fossil taxa within Ornithuromorpha, in which specimens either preserve a ventrally projecting keel, as in *Gansus* and *Piscivoravis*[52,53], or a thick keel base, in which the keel has presumably broken off, as in *Iteravis* and *Bellulornis*[54–56] (based on the phylogenetic hypotheses presented by ref. 28). Although an enlarged sternum with a prominent keel in fossil taxa has been used to infer increased aerial capabilities, recent studies have proposed that stem birds lacking ossified sterna or large sternal keels may have instead flown using pectoral musculature that attaches onto gastralia[32,48] or other bones of the shoulder girdle[33]. Generally, progress in understanding the origins of the large, keeled sternum of Neornithes and its role in the evolution of modern avian flight has been limited by the absence of explicit, quantitative studies.

Here, we examine the evolution of the sternum across stem birds following the origins of vaned feathers, which is often used as a benchmark for the earliest point at which powered flight was possible[28], using phylogenetic comparative analysis and ancestral character estimation of sternum morphology. Specifically, we examine how key features of the sternum, including relative size, shape dimensions, midline fusion and a prominent keel evolved. Analysing these evolutionary patterns of the sternum fills a substantial gap in our understanding of modern avian flight origins in the fossil record.

Results

Sternum morphometrics and ancestral character estimation

To examine both allometric and evolutionary patterns in sternum morphology, we compared a series of multivariate phylogenetic regression models analysing various metrics of sternum morphology, size variables and locomotor traits in extant birds, as well as ancestral character estimations to trace sternal trait acquisition through the stem avian lineage.

Sternum plate area. For extant-only data, the optimal model was 'sternum plate area ~ body mass + forelimb propulsion + aerial flight + foot-propelled swimming and diving + cursoriality' (Fig. 2a and Supplementary Table 1). This relationship is similar to that found in the 'sternum centroid ~ body mass' regression of refs. 6,43, suggesting that there is similar ecomorphological signal in the two-dimensional (2D) 'footprint' (lacking the keel area) as is found in the entire three-dimensional (3D) sternum among extant birds. Residual plots show that extant flightless birds have smaller sterna on average compared with other flight categories (Fig. 2b). Early diverging fossil taxa such as oviraptorosaurs and dromaeosaurids (except for *Microraptor*) show the largest residuals below the regression line for extant taxa, indicating that they have smaller sterna relative to body mass. Fossil taxa from the bird stem lineage at Pygostylia (*Jinguofortis perplexus*) and descendants fall within range of extant birds. Ancestral reconstructions of relative sternum area (residuals from the best-supported model) show notable increase in relative size at the base of Avialae, and another distinct increase at crownward Ornithuromorpha, reconstructed at the shared ancestor of *Gansus* and Songlingornithidae (represented by *Piscivoravis* in our dataset), using both the minimum and maximum body mass estimates (Fig. 3).

Minimum sternum length. The optimal model for minimum sternum length (length from base of craniolateral processes to cranial-most point of the sternal notch) was: 'minimum sternum length ~ body mass + forelimb propulsion + aerial flight + burst flight' (Supplementary Fig. 4a and Supplementary Table 5). Since the sternal morphology associated with burst flight is not representative of the ancestral sternal morphology for Neornithes[6], the regression line was drawn such that burst flight was set to 0, while the other variables were set to 1. This adjusts the intercept of the line, but not the slope. Burst fliers have much shorter minimum sternal lengths than any other flight group, as they have long lateral trabeculae[6] that are not included in the minimum sternal length index. Minimum lengths for flightless extant birds do not differ substantially from other flight groups (aside from burst fliers) (Supplementary Fig. 4b). Minimum sternum lengths in fossil taxa are highly variable throughout Paraves, with notably larger relative lengths within Microraptorinae, and an additional increase at Ornithuromorpha (Supplementary Fig. 5a,b).

Maximum sternum length. The optimal model for maximum sternum length (total sternum length) was: 'maximum sternum length ~ body mass + forelimb propulsion + aerial flight + burst flight' (Supplementary Fig. 6a and Supplementary Table 6). Maximum sternal length is much larger in burst fliers compared with other flight groups, which is opposite from the pattern observed in minimum sternal length. Most fossil groups show similar maximum to minimum sternal length as many do not have lateral and/or intermediate trabeculae, and those in fossils that do are shorter than in many extant birds. Fossils within Pygostylia show relative maximum sternal lengths comparable with flying birds (Supplementary Fig. 6b). Maximum sternum length increases substantially at the ancestor of Pygostylia and with a second increase in crownward Ornithuromorpha (Supplementary Fig. 7a,b).

Sternal dimensions. To assess evolutionary patterns of sternal elongation, we constructed a model with maximum sternum length as the *y* variable and sternum width as the *x* variable, omitting body mass from the model. The optimal model was: 'maximum sternum length ~ sternum width + forelimb propulsion + aerial flight + terrestriality + cursoriality' (Fig. 4a and Supplementary Table 7). Neornithine sterna appear to be more elongated than all fossil sterna and extant burst fliers have longer sterna relative to width compared with other locomotor groups. However, no other locomotor group (including flightless birds) shows distinct relative length to width patterns (Fig. 4b). All fossil taxa have smaller sternal lengths relative to their widths than do extant birds, with broader, shorter sterna in oviraptorosaurs and dromaeosaurids. There is a distinct increase in length relative to width in Ornithothoraces, where sternal elongation enters the range occupied by >75% of flying birds in Ornithothoraces (Fig. 4c).

Discrete ancestral character estimation. Discrete traits—midline fusion of sternal plates and the state of the keel—were subjected to ancestral character estimation to examine their evolutionary patterns. These analyses incorporated three additional fossil taxa that are known to lack ossified sternal remains to calibrate ancestral estimations: *Archaeopteryx lithographica*, *Anchiornis huxleyi* and *Sapeornis chaoyangensis*. Model selection using Akaike's information criterion corrected for small sample sizes (AICc) was implemented to identify the best-fit Markov *k* model[57] of discrete character evolution for the two discrete characters being analysed. For midline fusion of the sternum, an equal rates model of trait evolution was favoured. Our reconstructions estimate an ossified, unfused two-plate sternum at the ancestor of Pennaraptora, the loss of an ossified sternum at the ancestor of Avialae and a medially fused sternum at the most recent common ancestor of Pygostylia, with an independent loss of an ossified sternum in *Sapeornis* (Fig. 5a). For keel evolution, a custom discrete character matrix model was favoured. An entirely absent keel on an ossified sternum is reconstructed at the ancestor of Pennaraptora, while the loss of an ossified sternum is reconstructed at the ancestor of Avialae ~55% of the time and ~40% a keel-less, ossified sternum. A low, ridge-like keel is reconstructed ~50% of the time at the ancestor of Pygostylia, with a keel-less ossified sternum and an absent

https://doi.org/10.1038/s41559-025-02795-4

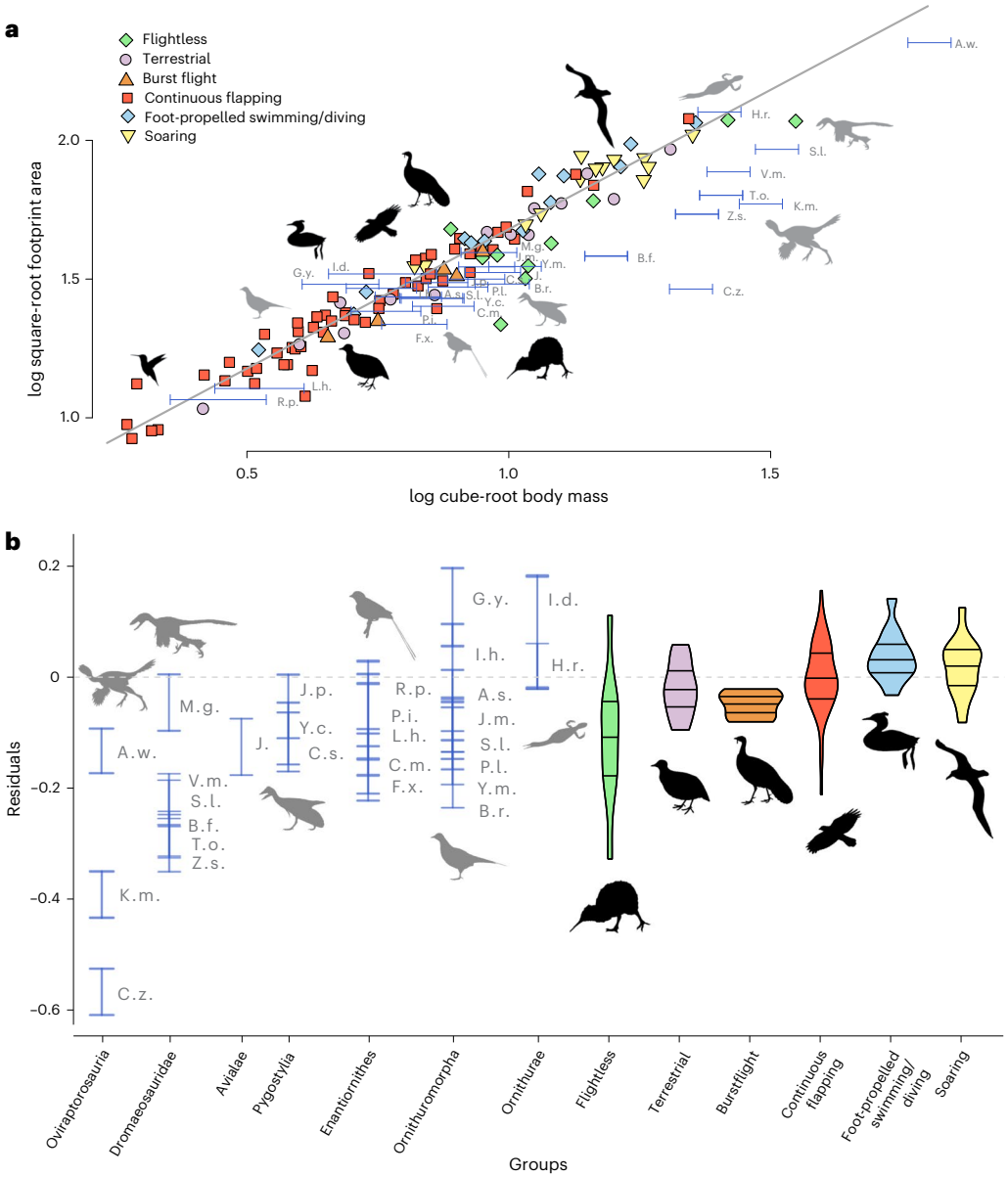

Fig. 2 | Phylogenetic generalized least squares analysis of relative sternum plate area (n = 112 extant taxa; n = 28 fossil taxa). a, Sternum footprint area plotted against log-transformed body mass (g) for both extant and fossil taxa, with regression line representing best-fit model. Fossils are shown as error bars representing their minimum and maximum body mass estimates. Regression statistics provided in Supplementary Table 1. **b**, Residual values from **a**, showing minimum and maximum body mass ranges for fossils. Fossil taxon names are: A.s., *Archaeorhynchus spathula*; A.w., *Anzu wyliei*; B.f., *Bambiraptor feinbergi*; B.r., *Bellulornis rectusunguis*; C.s., *Confuciusornis sanctus*; C.m., *Chiappeavis magnapremaxillo*; C.z., *Caudipteryx zoui*; F.x., *Fortunguavis xiaotaizicus*; G.y., *Gansus yumenensis*; H.r., *Hesperornis regalis*; I.d., *Ichthyornis dispar*; I.h., *Iteravis huchzermeyeri*; J., *Jeholornis*; J.m., *Jianchangornis microdonta*; J.p., *Jinguofortis perplexus*; K.m., *Khaan mckennai*; L.h., *Longirostravis hani*; M.g., *Microraptor gui*; P.i., *Piscivorenantiornis inusitatus*; P.l., *Piscivoravis lii*; R.p., *Rapaxavis pani*; Sa.l., *Sauronitholestes langstoni*; Sc.l., *Schizoura lii*; T.o., *Tianyuraptor ostromi*; V.m., *Velociraptor mongoliensis*; Y.c., *Yangavis confucii*; Y.m., *Yanornis martini*; Z.s., *Zhenyuanlong suni*. Credit: Silhouettes from Phylopic (http://phylopic.org/) under a Creative Commons license: *Archilochus colubris* and *Accipiter cooperii*, Andy Wilson (CC0 1.0); *Yixianornis grabaui* and *Protopteryx fengningensis*, Matt Martyniuk (CCBY 3.0); *Podiceps cristatus*, *Diomedeidae* and *Apteryx*, Ferran Sayol (CC0 1.0); *Meleagris ocellata* and *Pedionomus torquatus* (PDM 1.0); *Hesperornis regalis*, Nobu Tamura and T. Michael Keesey (CCBY 3.0); *Confuciusornis sanctus*, Scott Hartman (CC BY 3.0); *Luoyanggia liudianensis*, Brad McFeeters and T. Michael Keesey (CC0 1.0); *Sinornithosaurus millenii*, Scott Hartman and T. Michael Keesey (CC BY SA 3.0).

sternum each reconstructed here at ~40% and ~10%, respectively. By the Ornithothoraces node, this low ridge-like keel is reconstructed 100% of the time. A prominent keel is reconstructed ~95% of the time at the ancestor of crownward Ornithuromorpha, including *Piscivoravis* onwards (Fig. 5b).

Discriminant analysis

To estimate the predictive power of sternum morphology for flight abilities, we performed a phylogenetic flexible discriminant analysis (pFDA) on the relative size of sternum footprint area to body mass. The posterior correct classification rate (CCR) for inferring forelimb propulsion ability in Neornithes from relative footprint area was 0.85 (0.7–0.95 CCR), indicating that sternal footprint area has high predictive power for flight ability within the bird crown group. The pFDA estimated generally higher probabilities for presence of flight ability when estimates incorporated minimum rather than maximum body mass estimates (Extended Data Fig. 1 and Supplementary Table 8). Oviraptorosaurs and dromaeosaurids (except for *Microraptor*) yielded

https://doi.org/10.1038/s41559-025-02795-4

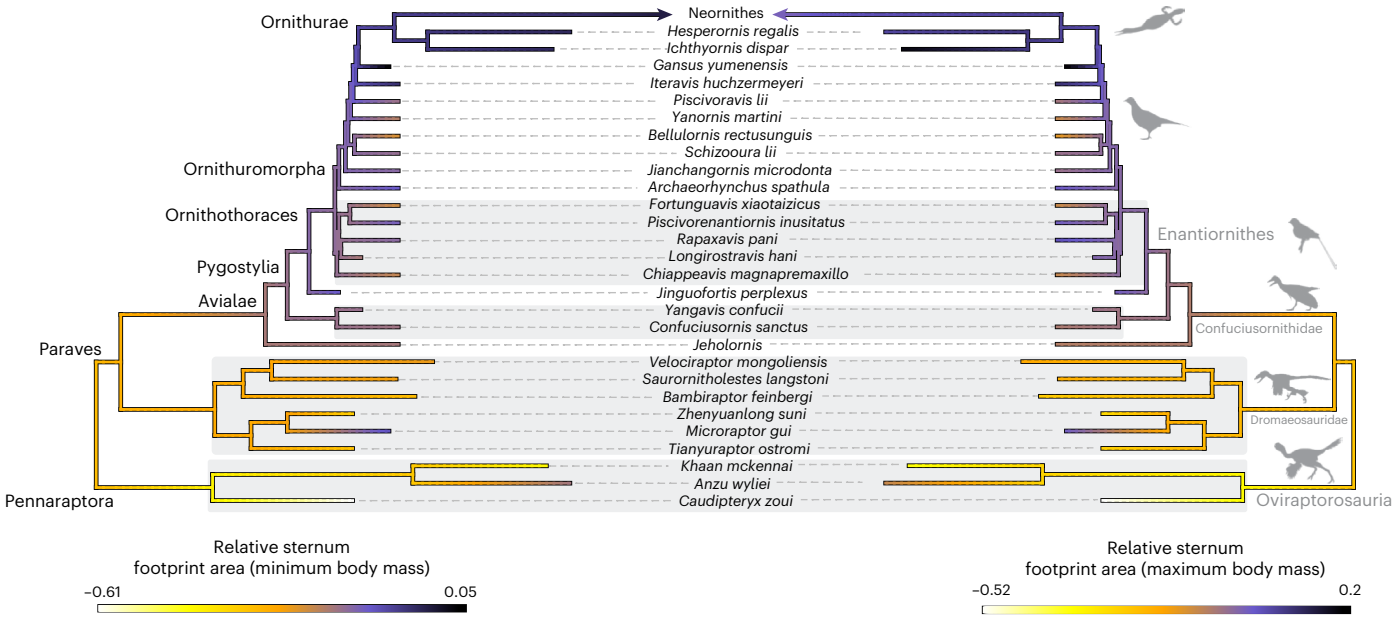

Fig. 3 | Ancestral character estimation of relative sternum plate area. Analyses based on minimum (left) and maximum (right) body mass estimates for fossil taxa ($n = 112$ extant taxa; $n = 28$ fossil taxa). For visualization purposes, the extant portion of the tree was condensed into a single branch labelled 'Neornithes', setting the tip value at 0, which represents the relative value for the ancestor of the living bird crown group, Neornithes. Credit: Silhouettes from Phylopic (http://phylopic.org/) under a Creative Commons license: *Y. grabaui* and *P. fengningensis*, Matt Martyniuk (CC BY 3.0); *H. regalis*, Nobu Tamura and T. Michael Keesey (CC BY 3.0); *C. sanctus*, Scott Hartman (CC BY 3.0); *L. liudianensis*, Brad McFeeters and T. Michael Keesey (CC0 1.0); *S. millenii*, Scott Hartman and T. Michael Keesey (CC BY SA 3.0).

unequivocal absence of flight ability. Results from different body mass estimates for *Microraptor* differed drastically, with minimum body mass yielding a median probability of 0.76 presence (forelimb propulsion probably present) while maximum body mass yielded a median probability of 0.49 (in the range of uncertainty). Estimates for *Confuciusornis* indicate that forelimb propulsion is probably absent regardless of body mass estimate (probability from minimum body mass, 0.38; probability from maximum body mass, 0.3). There is substantial variation in probabilities across Avialae. Crownward Ornithuromorpha present nearly unequivocal evidence for the presence of forelimb propulsion in *Iteravis*, *Gansus* and *Ichthyornis*, indicating that these taxa possess a relative sternum footprint area that is large enough to have had the potential to sustain forelimb-driven propulsion and potentially powered flight (Extended Data Fig. 1). The estimates for *Hesperornis* sit near the borderline for the presence of forelimb propulsion when both minimum ($P = 0.6$) and maximum ($P = 0.66$) body mass are considered. Ancestral character estimation of median flight probability shows the ancestor of Pennaraptora having a very low probability of forelimb propulsion ability, which increases to moderate at the ancestor of Avialae, within the zone of uncertainty (ancestral median probabilities across Avialae $P = 0.32–0.65$). Ancestral probabilities begin to suggest the presence of forelimb propulsion at the ancestor of crownward Ornithuromorpha when both minimum and maximum body mass estimates are incorporated (Extended Data Fig. 2a,b).

Discussion

The evolutionary patterns of functionally important traits, such as sternum morphology, are key to reconstructing the sequence of trait acquisition that led to the origin of flight along the avian lineage. We found that sternum evolution is characterized by two distinct episodes of modification, first at the base of Pygostylia and again within Ornithuromorpha. Further, after removing the dorsoventral dimension encompassing the keel to obtain the sternal footprint, we find similar ecomorphological patterns in the 2D keel-less 'footprint' as are found in the entire 3D sternum (Fig. 2a and Supplementary Fig. 9). The flightless diving *Hesperornis* is a known exception, likely to be secondarily flightless owing to its lack of a keel and distinct aquatic adaptations[58], despite being reconstructed here as possibly capable of flight on the basis of sternum size. This reinforces that the keel works in concert with the rest of the morphologically complex sternum to facilitate locomotion[6,43,59,60].

Our analyses support previous findings that flightless neornithine birds have proportionally smaller sterna than flying birds[6]. These small relative sizes are also found in oviraptorosaurs and most dromaeosaurids (Fig. 2b), suggesting that their sterna are too small to sustain neornithine-like flight. There are subsequently two distinct episodes of proportional sternum size increase: once in Avialae and again within Ornithuromorpha (Fig. 3). The sternum of the dromaeosaurid *Microraptor* is similar in proportional size to that of pygostylians, but it is much smaller in other dromaeosaurids. While our analyses suggest a single origin of an enlarged fused sternum within Avialae, specifically at the ancestor of *Jeholornis* + Pygostylia, it is likely that this also evolved in parallel in *Microraptor*. Basal avialans and *Microraptor* are the earliest taxa to show proportional sternum sizes within range of flying neornithines, comparable to continuous flappers (Fig. 2). Further, the highest rates of pectoral girdle evolution occur along the stem lineage at Avialae[61], with similarly high rates along the early branches of Ornithothoraces (Enantiornithes + Ornithuromorpha). Higher pectoral evolutionary rates at Avialae imply entry into a new adaptive zone, such as volancy or arboreality[15,62], which was probably facilitated by a larger sternum. Additional bird-like modifications occurring in this group, including the emergence of a low ridge keel in Confuciusornithidae (Figs. 5b and 6), craniocaudal elongation of the sternum (Figs. 4 and 6) and a cranial shift in centre of mass[63,64] (Fig. 6), suggest a pivotal moment in neornithine-like flight evolution.

Sternum size increased again within Ornithuromorpha at the ancestor of *Iteravis* + Ornithurae (Figs. 3 and 6), co-occurring with the transition from a low midline ridge to a fully developed sternal keel (Fig. 6). Taxa in this group also possess enlarged lateral trabeculae,

https://doi.org/10.1038/s41559-025-02795-4

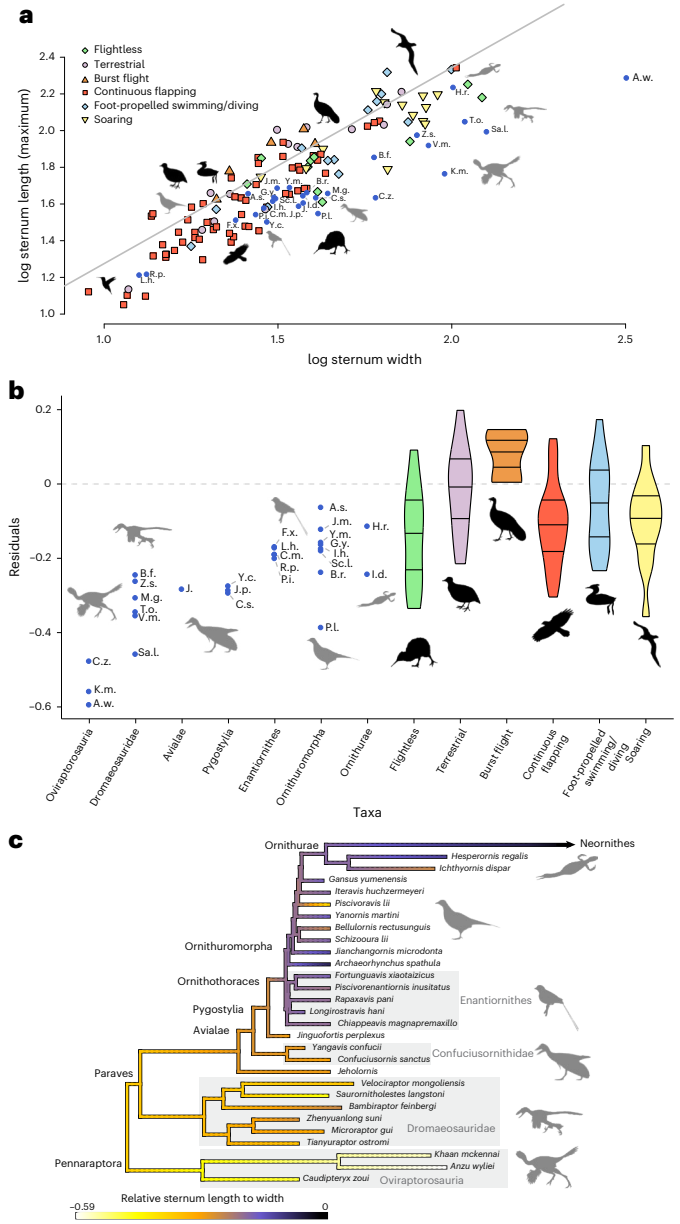

Fig. 4 | Phylogenetic generalized least squares analysis of sternum length relative to width (n = 112 extant taxa; n = 28 fossil taxa). a, Maximum sternum length plotted against sternum width for extant and fossil taxa, with regression line representing the best-fit model. Regression statistics provided in Supplementary Table 7. **b**, Residual values from **a**. **c**, Ancestral character estimation based on residual values from the regression shown in **a**. The extant portion of the tree was condensed into a single branch labelled 'Neornithes', setting the tip value at 0, which represents the relative value for the ancestor of the living bird crown group, Neornithes. Fossil taxon abbreviations in **b**, as given in Fig. 2. Credit: Silhouettes from Phylopic (http://phylopic.org/) under a Creative Commons license: *A. colubris* and *A. cooperii*, Andy Wilson (CC0 1.0); *Y. grabaui* and *P. fengningensis*, Matt Martyniuk (CC BY 3.0); *P. cristatus*, *Diomedeidae* and *Apteryx*, Ferran Sayol (CC0 1.0); *M. ocellata* and *P. torquatus* (PDM 1.0); *H. regalis*, Nobu Tamura and T. Michael Keesey (CC BY 3.0); *C. sanctus*, Scott Hartman (CC BY 3.0); *L. liudianensis*, Brad McFeeters and T. Michael Keesey (CC0 1.0); *S. millenii*, Scott Hartman and T. Michael Keesey (CC BY SA 3.0).

which along with the sternal keel are crucial areas of flight muscle attachment in Neornithes. This indicates that, while these muscles were involved in powered flight from their earliest forms[48], their anchor-points became larger and sturdier over time. Thus, while early beginnings of powered flight probably occurred in Avialae, advanced neornithine-like powered flight became prevalent within crownward Ornithuromorpha.

Some cases of a small sternum footprint area combined with a fully formed sternal keel suggest the potential for trade-offs in muscle attachment area. In the ornithuromorphs *Bellulornis* and *Piscivoravis*, the sternum footprint areas are small such that the discriminant function estimates them as flightless despite their developed keels[53–55]. Given the importance of a keel for flight[5,65], smaller sternal footprint areas in birds that evolved after the appearance of a fully formed keel probably do not indicate flightlessness, but that the development of the keel may be associated with an initial minor reduction in sternum footprint size, before further increasing in crownward ornithuromorphs such as *Iteravis* and *Gansus*. Further, *Bellulornis* and *Piscivoravis* show substantial evidence for wing and tail feathers[53,54], which are the main lines of evidence for their powered flight abilities. Nevertheless, the relative footprint areas of these basal ornithuromorphs fall mainly within the lower range of living birds such that they may be interpreted as flightless if relying on sternum footprint area alone (Fig. 2b). Therefore, while sternum size proves to be useful to infer flight capabilities, it should be considered in concert with other anatomical features.

An enlarged and ossified keel, from which the major flight muscles originate, is tightly correlated with forelimb-driven propulsive locomotion in birds[6,43], as supported by our extant-only tests of keel area (Supplementary Fig. 1). The supracoracoideus muscle in Neornithes, which lifts the wing dorsally, originates at the base of the sternal keel with a tendon that passes through the triosseal canal to attach onto the humerus[66,67]. In contrast, the more powerful pectoralis muscle lowers the wing in downstrokes, and originates both from the furcula and the most ventral portion of the ossified keel, as well as the lateral sides of the lateral trabeculae[65,68,69]. In living birds, the depth of the keel is more strongly associated with the size of the supracoracoideus than the pectoralis, and the supracoracoideus is vital for both strong flapping flight and ground take-off while a shallow keel is generally associated with less manoeuvrability and flight control[65,70–73]. We show that soarers and foot-propelled swimmers have smaller keels relative to sternum footprint size compared with continuous flappers and burst fliers (Supplementary Fig. 1d), as they often use external forces, such as thermal updraughts or water pressure to maintain buoyancy, and require less muscle power[74,75]. The low ridge-like keel in confuciusornithids may point towards the beginnings of the supracoracoideus muscle attaching onto the sternal keel; however, a triosseal canal is not found in any confuciusornithid, and definitive evidence of the structure is seldom found in fossils[5,72,76] (but see proposed triosseal canals in *Sapeornis*, *Jeholornis* and *Piscivorenantiornis* in ref. 41). This midline ridge in *Confuciusornis* may also suggest further cartilaginous extension acting as a keel, which had not ossified as a result of low muscular stress[77], and evidence of pectoral soft-tissues and a large deltopectoral crest in *Confuciusornis* suggests stable soaring rather than high-speed flight[78]. This suggests that rudimentary, non-neornithine-like volancy was still possible with a low ridge in place of a keel in basal pygostylians, such as *Confuciusornis*, although this was probably not manoeuvrable or sustained flight[5,10,33,71,79]. This is corroborated by our analysis of skeletal proportions, which suggests possible flight ability in *Confuciusornis* based largely on their appendicular skeleton anatomy without considering the sternum. Further, analyses of claw curvature suggest that *Confuciusornis* possibly had greater tree-climbing abilities than *Microraptor*[80], which may have facilitated the ability to glide before the evolution of flapping abilities. In contrast, the slight elongation of the *Microraptor* sternum, combined with the absence of a keel, suggests greater pectoralis rather than supracoracoideus action at this stage, which may be more consistent with basic flight abilities rather than tree-climbing before Avialae. This would be consistent with previous hypotheses that the supracoracoideus originated from elsewhere than the sternum, such as the coracoid, in dromaeosaurids[5,81].

https://doi.org/10.1038/s41559-025-02795-4

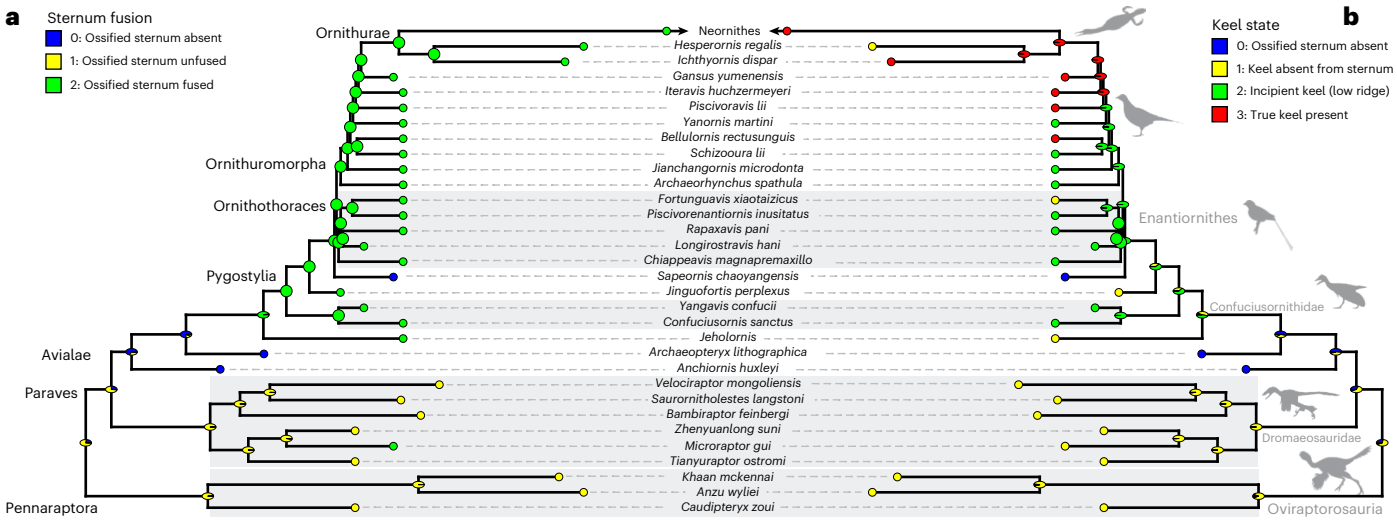

Fig. 5 | Ancestral state estimation of discrete sternal traits (n = 112 extant taxa; n = 31 fossil taxa). a, Midline fusion of the sternum. **b**, Sternal keel development. The extant portion of the tree was condensed into a single branch labelled 'Neornithes', setting the tip value at 0, which represents the relative value for the ancestor of the living bird crown group, Neornithes. Credit: Silhouettes from Phylopic (http://phylopic.org/) under a Creative Commons license: *Y. grabaui* and *P. fengningensis*, Matt Martyniuk (CCBY 3.0); *H. regalis*, Nobu Tamura and T. Michael Keesey (CC BY 3.0); *C. sanctus*, Scott Hartman (CC BY 3.0); *L. liudianensis*, Brad McFeeters and T. Michael Keesey (CC0 1.0); *S. millenii*, Scott Hartman and T. Michael Keesey (CC BY SA 3.0).

The second sternum size increase, combined with the appearance of a fully developed keel in crownward Ornithuromorpha, implies a substantial leap towards neornithine-like flight capabilities at this node. However, fragmentary sterna from Late Cretaceous enantiornithines, such as *Neuquenornis*[51], *Enantiornis*[82] and *Mirarce*[83], clearly show developed sternal keels, suggesting that the first fully formed ossified keels evolved independently of Ornithuromorpha. Owing to their fragmentary nature, these fossils were not included in these analyses. However, other flight-related sternal modifications appear in enantiornithines, such as long lateral trabeculae in *Rapaxavis* and *Chiappeavis*. This suggests that, while crownward ornithuromorphs possess the appropriate combination of traits for sternum-anchored flight, there were probably a few evolutionary experiments for flight adaptations within Enantiornithes as well. Furthermore, it is not always obvious whether a low midline ridge represents the full keel morphology in that taxon, the base of a cartilaginous keel or a fully developed keel that has broken off, given the variable wear patterns on broken fossil surfaces. Recently discovered fossils of flying passerines show sterna with low ridge keels[84], in which there is no doubt that a fully developed keel had been present in these taxa before fossilization and had since broken off. A more in-depth taphonomic study of broken keels in flattened fossil birds and keel surface topography may be necessary to properly interpret this variation in fossilized keels.

Burst flight, a highly specialized form of escape flight in Neornithes, is associated with extremely narrow and elongated sterna[6] (Fig. 4). While this could be hypothesized as a plesiomorphic step towards flapping flight, fossil sterna never reach the extreme elongated condition occupied by extant burst fliers. Therefore, we cannot infer burst flight as an ancestral or transitional behaviour in the evolution of powered flight on the basis of skeletal morphology alone; however, this does not rule out the possibility of comparable locomotor behaviours in fossil taxa with different musculoskeletal arrangements[42]. The distinction between our results from the minimum and maximum sternum lengths is indicative of variation in length of the lateral and intermediate trabeculae, with the longest trabeculae occurring in extant burst fliers (Supplementary Figs. 4 and 6). These trabeculae vary immensely across living birds and are often covered by connective tissue, which further contributes sternal attachment area for the pectoralis muscle and by extension increases the potential downstroke force[35,67]. Through the stem lineage, trabeculae only appear in Ornithothoraces, which show variable lengths across Enantiornithes and Ornithuromorpha (Supplementary Figs. 5 and 7), probably indicating an additional step towards stronger flapping ability. The absence of trabeculae in basal avialans suggests limited downstroke capacity, despite the increase in relative sternum sizes and appearance of a low midline ridge in Avialae that suggest early flight potential. This further indicates that basic flight capabilities emerging in basal Avialae were limited, although such abilities could have been compensated for with elongated forelimbs, as observed in *Confuciusornis*[42,85].

These results propose two distinct episodes of sternal modification in the lineage leading to crown-group birds. The first episode involves an increase in relative sternum size and midline fusion of sternal plates in Avialae, followed by the appearance of a rudimentary keel in basal Pygostylia (Fig. 5a). A large, fused sternum is present in the non-avialan dromaeosaurid *Microraptor* and no other dromaeosaurids, suggesting that *Microraptor* was an evolutionary experiment before the proliferation of these traits in Avialae. This supports the hypotheses that *Microraptor* evolved some form of volant locomotion independently[28]. The basal avialans *Archaeopteryx* and *Anchiornis*, and the pygostylian *Sapeornis*, conspicuously lack ossified sternal remains[32], and are the only taxa with enough evidence to both (1) refer to the taxonomic position of basal Avialae[28,62] and (2) ascertain that they lack sternal ossifications, as each taxon is known by several body fossil specimens of exceptional preservation[32,86–88]. When these sternum-less taxa are included in our ancestral estimations of sternal fusion and keel evolution, they strongly influence the value at the ancestral node of Avialae, which is estimated to lack an ossified sternum. This total loss of a sternum at a pivotal moment in flight evolution is unlikely given the presence of several other flight-related traits, such as feathered wings, elongated forelimbs and reduced manual digits[32,87,89,90]. However, this does suggest potential experimentation with a cartilaginous sternum, which, combined with ossified gastralia, may have anchored the pectoral muscles in early manifestations of volancy[32,48]. Further, the sternum becomes markedly more elongated in Pygostylia (Fig. 4), indicating that the sternum size increase at Avialae is not simply an artefact of sternal elongation. The second episode of sternum-anchored flight evolution occurs in crownward

https://doi.org/10.1038/s41559-025-02795-4

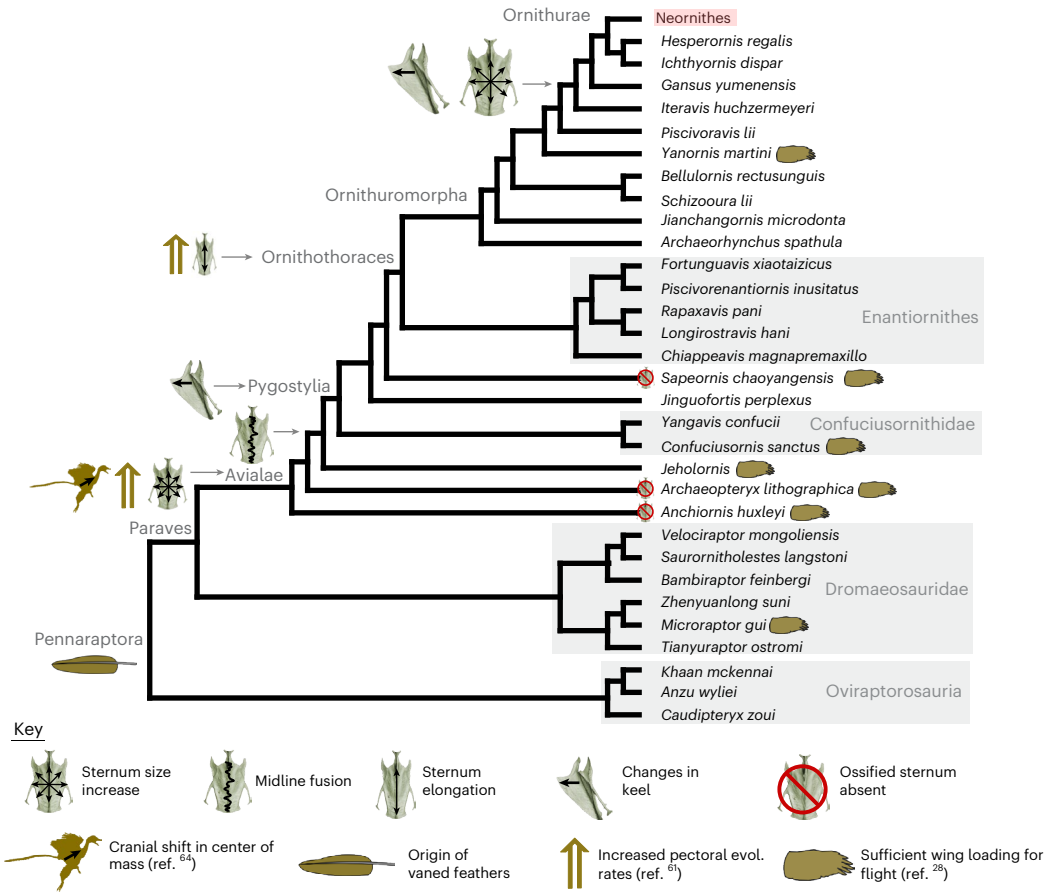

Fig. 6 | The evolution of the sternum across the dinosaur–bird transition. Synthesis based on broad conclusions from this study and those from other recent papers on avian flight evolution. Credit: Silhouettes from PhyloPic (https://www.phylopic.org/) under a Creative Commons license: *Archaeopteryx lithographica*, T. Michael Keesey (CC0 1.0).

Ornithuromorpha, coinciding with an increase in sternum width (Supplementary Fig. 3), enlarged lateral trabeculae (Supplementary Fig. 7) and a fully developed keel (Fig. 5b), the last two being crucial areas of flight muscle attachment. Ornithuromorphs are known for their many derived flight characteristics shared with living birds, including lateral wing folding capabilities[91], a prominent extensor process on the carpometacarpus characteristic of automated wing extension[92,93] and a tail feather fan facilitated by a specialized pygostyle morphology[94].

These two evolutionary events, defined by several morphological transitions clustered within short taxonomic spans, suggest that selective pressures for flight abilities were particularly strong for early members of these two groups. Basal avialans *Archaeopteryx* and *Anchiornis* are suggested to have been primarily ground-dwelling[95], while more aerial and arboreal tendencies have been identified in the pygostylians *Confuciusornis* and *Sapeornis*[80,95,96] and Ornithuromorpha has been suggested to represent a transition to terrestrial lifestyle from the arboreal Enantiornithes[10,97]. Further macroevolutionary analyses of the ecology of these stem birds can elucidate the selective pressures shaping their morphology. Estimating flight ability in fossils using linear skeletal proportions produced primarily ambiguous results in most fossil taxa, with flight ability estimated as being present only in confuciusornithids. This result conflicts with our sternum analysis, in which relative sternum size in confuciusornithids predicted a lack of neornithine-like powered flight ability, while such ability was predicted to be present in other fossil taxa with larger sterna, such as *Rapaxavis*. This further suggests that no single anatomical structure can be used to confidently infer flight behaviours in fossil taxa, as development of one area over evolutionary time—sternal keel and appendicular proportions, in this case—may compensate for deficiencies in other flight features, such as a small sternum footprint. Confuciusornithids, which have much longer forelimbs relative to their hindlimbs, present a mixture of advanced and underdeveloped features[85]. Combined with the appearance of a low ridge keel in these taxa and a slightly enlarged sternum footprint, confuciusornithids clearly represent a pivotal moment in flight evolution. When this linear dataset was first implemented in ref. 43, the measurement with the greatest influence on overall variation was the depth of the sternal keel. This measurement could not be included in our fossil dataset, as most fossil sterna lack keels either fundamentally or through taphonomic destruction. While we attempted to replicate the measurement dataset from the previous study, the skeletal proportions dataset performs differently and unreliably when reconstructing flight abilities without this sternal keel measurement.

Major evolutionary transitions are defined by entry into new ecological domains, often observed through a complex suite of morphological traits. This study shows that sternum morphology provides insights into the pattern of neornithine-like flight evolution. The evolution of the sternum, the central portion of the flight apparatus, was episodic, before becoming highly specialized for modern bird flight. Early manifestations of flight were probably highly constrained by limited muscular power, body size and a lack of derived skeletal specializations[91], such as a sufficiently large sternum size relative to body size. The pectoralis-dominated powered flight that is characteristic of living birds began to assemble in Avialae and was probably fully developed in crownward Ornithuromorpha, with a few evolutionary experiments along the way. Not only is the sternal keel critical for neornithine-like powered flight, but the lateral and

intermediate trabeculae are probably underappreciated in determining flight capabilities, and variation in this morphology should be investigated further in future studies.

Methods

Data acquisition and processing

We analysed various aspects of the sternum morphology in a comparative framework across a broad sample of pennaraptoran dinosaurs, stem birds and modern birds (Fig. 1). These indices (sternum plate area in millimetres squared (mm^2), width, minimum length and maximum length in mm; described further below) were selected to allow comparisons between extant bird specimens and fossil sterna, which are often flattened and many of which are visible only in ventral view. The extant dataset consisted of 3D renderings (either from computed tomography or surface scans) of sterna from 112 living bird species across 62 neornithine families, sourced from ref. 43. We also assembled a dataset of 28 fossil sterna from taxa across Pennaraptora, selecting specimens with the most adequate preservation of a complete sternum or sternal plates (Fig. 1). Three fossil taxa that are well-represented in the fossil record without any ossified sternal remains (*Archaeopteryx lithographica*, *Sapeornis chaoyangensis* and *Anchiornis huxleyi*) were included to calibrate ancestral state reconstructions of discrete traits. These three sternum-less taxa were selected on the basis of their overwhelmingly strong representation in the fossil record of specimens lacking sterna[88,98,99]. Although there are other paravian specimens that lack sterna, we cannot definitively conclude that these taxa lack sterna because of their fragmentary record. Similarly, paravian specimens with sternal remains that were not included here are poorly preserved. Therefore, we are certain that the fossil taxa included in this study represent all known and best-preserved fossil taxa, or those for which we can confidently claim that they have no ossified sternum.

Sternal plate area. Because most bird fossils are found in flattened slabs, the sternum plate area was estimated on the basis of its 2D 'footprint'. Fossil sterna were compared directly with those of extant birds from ref. 43 by projecting the 3D sternal landmarks from the extant dataset into the 2D plane defined by craniocaudal length and mediolateral width, while removing the dorsoventral dimension that encompasses the sternal keel. This was achieved by running a principal component analysis (PCA) to align the shape data and then removing the third (or *Z*) dimension representing depth in coordinate shape space. This converts the 3D dataset into 2D, producing a sternum 'footprint' similar to those estimated in fossils. These 2D footprints slightly underestimate sternum plate size, as real sterna are curved in the third dimension. This would have the biggest biasing effect on species with proportionally large sterna, as these curve around the body wall the most. To examine if quantifiable morphological variation in the 2D sternal footprint differs substantially from that of 3D sternum morphology, we ran separate PCAs for 2D and 3D sternum data to compare the two morphospaces. We found minimal difference in their morphological variation, indicating that the 2D sternum footprint retains most of the variation in the entire sternum, making it a logical alternative for comparative analysis (Supplementary Fig. 9). For extant sterna, sternum area was measured using the polyarea function in the pracma R package[100]. For fossils, sternum footprint area was measured from photos using the freehand selection tool in Fiji[101]. Footprint area was then square-rooted and log-transformed, to make it comparable to linear measurements and to increase homoscedasticity.

Keel area. To assess the importance of the sternal keel, the area of the keel in the extant dataset was calculated in mm^2 by running a PCA to project the 3D keel landmarks into 2D (craniocaudal length and dorsoventral height), then measuring the projected area using the polyarea function. Keel area was square-rooted and log-transformed, to make it comparable to linear measurements and to increase homoscedasticity.

Sternum dimensions. Sternum dimensions are represented here as width and length measurements, to characterize the extent of sternum elongation. Width was measured as the maximum mediolateral width of both sternal plates combined, whether fused or unfused. 'Minimum sternum length' was included to represent the craniocaudal length of the sternum without the craniolateral processes or lateral trabeculae. This was measured as the distance between the base of the craniolateral process and the cranial-most point of the medial sternal notch. 'Maximum sternum length' was included to represent the maximum craniocaudal length of the sternum including all craniolateral processes and lateral and intermediate trabeculae. All three of these metrics were measured using the freehand straight-line tool in Fiji[101] and then log-transformed.

We calculated a range of body mass estimates in grams for each fossil taxon using a suite of equations available through the R package MASSTIMATE[102–107]. These equations were each developed to estimate the body mass of extinct bipedal dinosaurs on the basis of minimum femoral shaft circumference. Body masses were then cube-rooted, to make them comparable to other linear measurements and log-transformed to convert proportional differences into an arithmetic scale[108]. Subsequent analyses that could only incorporate a single body mass for each taxon were run twice, using the minimum and maximum body mass estimates for each fossil taxon.

Phylogenetic comparative analyses were performed using the composite extant avian tree from ref. 109, which combines the age estimates and topology from ref. 110 with the genus-level supertree distribution of ref. 111. An additional time-scaled phylogeny that incorporated the fossil taxa was constructed by stitching together a fossil tree at the base of the tree from ref. 109. This was done by constructing a backbone topology of fossil taxa from recent phylogenetic estimates[28,62] and estimated branch lengths by scaling the tree with first and last occurrence data for each taxon, using the DatePhylo function from the R package strap[112]. This tree was then stitched to the base of the extant tree for analyses that included both fossil and extant taxa.

Two discrete traits were also coded in all taxa: midline fusion of sternal plates and sternal keel state. These analyses included taxa without any sternal remains (*Archaeopteryx lithographica*, *Sapeornis chaoyangensis* and *Anchiornis huxleyi*), to provide important evolutionary context for ancestral character estimations of these discrete traits. Sternal fusion was coded with three states: 0, ossified sternum absent; 1, sternum ossified and unfused; and 2, sternum ossified and fused. Sternal keel state was classified on the basis of four states: 0, ossified sternum absent; 1, no evidence of a keel on ossified sternum; 2, presence of a ridge along the midline; and 3, a prominent keel. State 2 was coded on the basis of the presence of ridges that shows no breakage or rugosity, suggesting that no further ossified keel was present beyond this low ridge (for example, *Confuciusornis*). State 3 was coded on the basis of the presence of a 3D preserved keel (for example, *Gansus* and *Ichthyornis*), or the presence of a thick keel base, in which the keel has presumably broken off, signifying the thickness of the keel when present (for example, *Iteravis*). All living bird taxa coded as 2 (fused) for sternal fusion and 3 (prominent keel) for sternal keel state, except for ratites (*Apteryx owenii* and *Casuarius casuarius*), which were coded as 1 (keel absent) for sternal keel state.

The following locomotory categories were incorporated in analyses: forelimb-driven propulsion, aerial flight, foot-propelled swimming and diving, burst flight, sustained flight, soaring, flap-gliding, continuous flapping, terrestriality, cursoriality and manoeuvrability (explanations provided in Table 1 of ref. 6). 'Aerial flight' and 'forelimb propulsion' are separated to account for birds that engage in underwater forelimb propulsion for swimming, such as penguins, but are not capable of aerial flight. These different locomotory categories are not mutually exclusive, as taxa are known to perform more than one of the alternate modes and were coded as 'present' or 'absent' so that

several locomotory modes could be assigned per taxon. Categorization of each of these modes was compiled using Handbook of Birds of the World[113] and the Cornell Laboratory of Ornithology 'Birds of the World'[114] online databases.

Macroevolutionary analysis

Analysis of sternal morphology in relation to flight abilities in fossil taxa requires an understanding of which locomotor variables best explain sternum morphology in extant birds. To identify the optimal combination of locomotor modes that explain variation in each sternal metric among Neornithes, a series of phylogenetically corrected multiple regression models[115] using the pgls function in the caper R package[116] were produced, with locomotor variables described in ref. 6. This tested the proposed relationships of each sternal metric with species body mass and locomotor modes. We specifically evaluated models formulated as 'sternal metric X ~ body mass + sternum size + locomotor mode 1 + locomotor mode 2…' to assign multiple locomotor modes per species by coding them as 'present' or 'absent'. Models of different variable combinations were compared and the best-supported model was identified using AICc (refs. 117,118). Residual values from the model were then calculated from the best-fit regression line, to quantify patterns of relative variation after accounting for body size, as in refs. 119,120. For metrics that could be measured in fossils (that is, all metrics except for keel area), residuals were also computed for the fossils and then visualized to compare the deviation from the trend line along the bird stem lineage and among extant bird locomotor categories. Each of these metrics was individually analysed as the dependent variable with a combination of body mass and locomotor traits (Table 1 in ref. 6) as the predictor variables. Additionally, we examined sternal dimensions by testing models of 'maximum sternal length ~ sternal width + locomotor' traits to explore elongation-related changes[6,43].

For the residuals of all metrics, except for keel area, maximum likelihood ancestral character estimation[121,122] was performed following the protocols outlined in ref. 123. Continuous trait estimation was executed using the fastAnc function and continuous trait evolution was visualized using the contMap function in phytools[124]. Residuals from each of the preferred regression models were implemented as the continuous trait to estimate for ancestral values along the phylogeny. Keel area was not included because it is not measurable in nearly any of the fossil taxa, and thus not informative on sternal evolution in the fossil stem lineage.

We also estimated ancestral states for the two discrete traits, sternal fusion and keel state. For sternal fusion, models of morphological character evolution (equal rates, all rates different, symmetrical and irreversible models were compared using AIC to choose the best fit to the data. One-hundred stochastic character maps[125] were then generated using the make.simmap function in phytools[126], to visualize ancestral state changes over 100 replicates.

For the keel state character, the same model comparison was performed as above, with the inclusion of an additional custom model, in which most states can transition between one another, including the total loss of a keel (3 to 1), but not the transition from 3 to 2, as 2 represents a transitional phase in keel evolution, and is not interpreted to be homologous with a 'shallow' keel in extant birds (Supplementary Table 10). Similar to the above, 100 stochastic character maps were generated to visualize ancestral state changes over 100 replicates. For visualization purposes, the extant portion of the tree was condensed into a single branch labelled 'Neornithes', setting the tip value at 0, which represents the relative value for the ancestor of the living bird crown group, Neornithes.

Discriminant analysis using sternum shape

To obtain estimates of the probabilities of flight capabilities in the fossil taxa, a pFDA[127,128] was implemented, following the protocol outlined in refs. 43,129. First, AICc was used to perform a model comparison between the best-supported models for each sternal metric (for example, 'sternum plate area ~ body mass + locomotor' variables versus 'sternum width ~ body mass + locomotor' variables). This process favoured the sternum plate area model ('sternum plate area ~ body mass + forelimb propulsion + aerial flight + foot-propelled swimming and diving + cursoriality'; Results), indicating that the locomotor data provide a better explanation of sternal area than of the other sternal metrics. The discriminant function was then run using the residuals from this model for both extant and fossil taxa to predict the posterior probability of the presence of flight (PP_{flight}), which here is represented by the 'forelimb propulsion' trait variable in the model ('forelimb propulsion' is considered to be present in flightless penguins; see ref. 6).

To account for unequal representation of the forelimb propulsion variable across the extant dataset (forelimb propulsion absent, $n = 10$; present, $n = 102$), we subsampled the dataset at random for an equal number ($n = 10$) of taxa exhibiting 'presence' and 'absence' for flight, and ran 100 replicates of the pFDA so that the subsampled dataset for 'presence' was different each time. From this range of 100 estimates, we extracted the mean PP_{flight} value, as well as the first and third quartiles of PP_{flight} estimates. We considered a mean PP_{flight} of <0.33 as 'probably absent', PP_{flight} of >0.67 as 'probably present' and $0.33 > PP_{flight} > 0.67$ as uncertain or equivocal. Accuracy was evaluated through CCR for living bird taxa. Flight was considered to be reliably estimated if it showed a median CCR of 0.67 or higher. Both the CCR and PP_{flight} were considered when evaluating the pFDA predictions. Finally, ancestral character estimation of the mean flight probability was performed to map the probability of flight presence in each fossil on the phylogeny.

Discriminant analysis using skeletal proportions

Skeletal proportions, represented by linear measurements across the skeleton, are a more traditional kind of morphometric data used in ecomorphological analyses of birds[43,130–132]. Previous work[43] showed that sternum morphology and skeletal proportions have complementary ecomorphological associations, with 3D geometric shape of the sternum associated more with specific locomotor styles, while skeletal proportions show stronger correlations with flight itself ('aerial flight' and 'forelimb propulsion' traits). To compare the predictive power of sternum footprint area with skeletal proportions, we implemented a set of linear skeletal measurements for an additional pFDA to estimate the presence or absence of forelimb propulsion in stem bird fossil taxa. The taxon sample for this analysis differs slightly from the sternum analysis ($n = 145$ extant taxa; $n = 15$ fossil taxa) because of the high-quality data availability; it was challenging to find fossil taxa with a sufficient set of skeletal measurements preserved, and impossible to measure the full set of skeletal measurements used for living birds[43] in almost any fossil species. Further, the set of measurements used here is reduced from those in the original study[32]. However, the datasets reflect similar taxonomic breadth as the sternum analysis. Here, we implemented the following 13 measurements for fossil taxa: humerus length, humerus proximal width, ulna length, radius length, carpometacarpus length, carpometacarpus proximal width, synsacrum length, ilium length, ischium length, pubis length, femur length, tibiotarsus length and tarsometatarsus length. Fossils were measured at the Institute of Vertebrate Palaeontology and Palaeoanthropology when available and measurements were otherwise recorded using the freehand line tool in Fiji[101]. Measurements were log-transformed and subjected to Mosimann's transformation, which computes size-corrected geometric shape vectors for each taxon by subtracting the log-geometric size (calculated as the mean across all measurements) from the log-transformed measurements[133]. We then tested the relationship between skeletal proportions and locomotor modes[6,43] using distance-based PGLS models[134] to choose

the best-fit model to calculate regression scores from the pFDA. The best-fit model was as follows: 'skeletal proportions ~ body size + aerial flight + forelimb propulsion + sustained flight + soaring + terrestriality + manoeuvrability'. We then conducted a pFDA on the regression scores from the best-supported model to predict the presence of the forelimb propulsion variable in the fossil taxa, with the same criteria described above.

Reporting summary

Further information on research design is available in the Nature Portfolio Reporting Summary linked to this article.

Data availability

Data generated and analysed in this study are available via Dryad at https://doi.org/10.5061/dryad.jsxksn0ng (ref. 135).

Code availability

R code for analyses performed here are available via Dryad at https://doi.org/10.5061/dryad.jsxksn0ng (ref. 135).

References

1. Hou, L., Martin, L. D., Zhou, Z. & Feduccia, A. Early adaptive radiation of birds: evidence from fossils from northeastern China. *Science* **274**, 1164–1167 (1996).
2. Chiappe, L. M. The first 85 million years of avian evolution. *Nature* **378**, 349–355 (1995).
3. Owen, R. *On the Anatomy of Vertebrates: Birds and Mammals* (Longmans, Green and Company, 1866).
4. O'Connor, J. K. et al. Evolution and functional significance of derived sternal ossification patterns in ornithothoracine birds. *J. Evol. Biol.* **28**, 1550–1567 (2015).
5. Mayr, G. Pectoral girdle morphology of Mesozoic birds and the evolution of the avian supracoracoideus muscle. *J. Ornithol.* **158**, 859–867 (2017).
6. Lowi-Merri, T., Benson, R. B. J., Claramunt, S. & Evans, D. C. The relationship between sternum variation and mode of locomotion in birds. *BMC Biol.* **19**, 165 (2021).
7. Nopcsa, B. F. Ideas on the origin of flight. *Proc. Zool. Soc. Lond.* **77**, 223–236 (1907).
8. Ostrom, J. H. Archaeopteryx and the origin of flight. *Q. Rev. Biol.* **49**, 27–47 (1974).
9. Padian, K. Cross-testing adaptive hypotheses: phylogenetic analysis and the origin of bird flight. *Am. Zool.* **41**, 598–607 (2001).
10. Zhou, Z. & Zhang, F. Mesozoic birds of China—a synoptic review. *Front. Biol. China* **2**, 1–14 (2007).
11. Lindsay, B. On the avian sternum. *Proc. Zool. Soc. Lond.* **53**, 684–716 (1885).
12. Zheng, X., Wang, X., O'Connor, J. & Zhou, Z. Insight into the early evolution of the avian sternum from juvenile enantiornithines. *Nat. Commun.* **3**, 1116–1118 (2012).
13. Lull, R. S. Volant adaptation in vertebrates. *Am. Nat.* **40**, 537–566 (1906).
14. Ridpath, M. The Tasmanian native hen, *Tribonyx mortierii*. III. Ecology. *CSIRO Wildl. Res.* **17**, 91–118 (1972).
15. Ostrom, J. H. Archaeopteryx and the origin of birds. *Biol. J. Linn. Soc.* **8**, 91–182 (1976).
16. Heimerdinger, M. A. & Ames, P. L. Variation in the sternal notches of suboscine passeriform birds. *Postilla* **105**, 1–44 (1967).
17. Feduccia, A. *The Origin and Evolution of Birds* (Yale Univ. Press, 1996).
18. Wang, M. & Zhou, Z. in *The Biology of the Avian Respiratory System: Evolution, Development, Structure and Function* (ed. Maina, J.) 1–26 (Springer, 2017).
19. Burgers, P. & Chiappe, L. M. The wing of Archaeopteryx as a primary thrust generator. *Nature* **399**, 60–62 (1999).
20. Dececchi, T. A., Larsson, H. C. E. & Habib, M. B. The wings before the bird: an evaluation of flapping-based locomotory hypotheses in bird antecedents. *PeerJ* **4**, e2159 (2016).
21. Heers, A. M., Baier, D. B., Jackson, B. E. & Dial, K. P. Flapping before flight: high resolution, three-dimensional skeletal kinematics of wings and legs during avian development. *PLoS ONE* **11**, e0153446 (2016).
22. Burnham, D. A. Archaeopteryx—a re-evaluation suggesting an arboreal habitat and an intermediate stage in trees down origin of flight. *Neues Jb. Geol. Paläontol. Abh.* **245**, 33–44 (2007).
23. Dial, K. P., Randall, R. J. & Dial, T. R. What use is half a wing in the ecology and evolution of birds? *Bioscience* **56**, 437–445 (2006).
24. Nudds, R. L. & Dyke, G. J. Forelimb posture in dinosaurs and the evolution of the avian flapping flight-stroke. *Evolution* **63**, 994–1002 (2009).
25. Senter, P. Scapular orientation in the theropods and basal birds, and the origin of flapping flight. *Acta Palaeontol. Pol.* **51**, 305–313 (2006).
26. Voeten, D. F. A. E. et al. Wing bone geometry reveals active flight in Archaeopteryx. *Nat. Commun.* **9**, 923 (2018).
27. Serrano, F. J. & Chiappe, L. M. Aerodynamic modelling of a Cretaceous bird reveals thermal soaring capabilities during early avian evolution. *J. R. Soc. Interface* **14**, 20170182 (2017).
28. Pei, R. et al. Potential for powered flight neared by most close avialan relatives, but few crossed its thresholds. *Curr. Biol.* **30**, 4033–4046 (2020).
29. Dial, K. P. Wing-assisted incline running and the evolution of flight. *Science* **299**, 402–404 (2003).
30. Jackson, B. E., Tobalske, B. W. & Dial, K. P. The broad range of contractile behaviour of the avian pectoralis: functional and evolutionary implications. *J. Exp. Biol.* **214**, 2354–2361 (2011).
31. Marsh, O. C. *Odontornithes: A Monograph of the Extinct Toothed Birds of North America* (G.P.O, 1880).
32. Zheng, X. et al. On the absence of sternal elements in Anchiornis (Paraves) and Sapeornis (Aves) and the complex early evolution of the avian sternum. *Proc. Natl Acad. Sci. USA* **111**, 13900–13905 (2014).
33. Pittman, M. et al. Preserved soft anatomy confirms shoulder-powered upstroke of early theropod flyers, reveals enhanced early pygostylian upstroke, and explains early sternum loss. *Proc. Natl Acad. Sci. USA* **119**, e2205476119 (2022).
34. Wang, X. et al. Basal paravian functional anatomy illuminated by high-detail body outline. *Nat. Commun.* **8**, 14576 (2017).
35. Zheng, X. et al. Structure and possible ventilatory function of unusual, expanded sternal ribs in the Early Cretaceous bird Jeholornis. *Cretac. Res.* **116**, 104597 (2020).
36. Hou, L.-H. et al. Confuciusornis sanctus, a new Late Jurassic sauriurine bird from China. *Chinese Sci. Bull.* **40**, 1545–1551 (1995).
37. O'Connor, J. K., Zheng, X.-T., Hu, H., Wang, X.-L. & Zhou, Z.-H. The morphology of *Chiappeavis magnapremaxillo* (Pengornithidae: Enantiornithes) and a comparison of aerodynamic function in Early Cretaceous avian tail fans. *Vertebr. Palasiat.* **55**, 41–58 (2017).
38. Wang, M., Oconnor, J. K. & Zhou, Z. A new robust enantiornithine bird from the Lower Cretaceous of China with scansorial adaptations. *J. Vertebr. Paleontol.* **34**, 657–671 (2014).
39. O'Connor, J. K., Chiappe, L. M., Gao, C. & Zhao, B. Anatomy of the early cretaceous enantiornithine bird *Rapaxavis pani*. *Acta Palaeontol. Pol.* **56**, 463–475 (2011).
40. Wu, Q., O'Connor, J. K., Wang, S. & Zhou, Z. Transformation of the pectoral girdle in pennaraptorans: critical steps in the formation of the modern avian shoulder joint. *PeerJ* **12**, e16960 (2024).
41. Wang, S. et al. Digital restoration of the pectoral girdles of two Early Cretaceous birds, and implications for early flight evolution. *eLife* 11, e76086 (2022).

42. Heers, A. M., Varghese, S. L., Hatier, L. K. & Cabrera, J. J. Multiple functional solutions during flightless to flight-capable transitions. *Front. Ecol. Evol.* **8**, 573411 (2021).
43. Lowi-Merri, T. M. et al. Reconstructing locomotor ecology of extinct avialans: a case study of Ichthyornis comparing sternum morphology and skeletal proportions. *Proc. R. Soc. B* **290**, 20222020 (2023).
44. Xu, X. et al. Four-winged dinosaurs from China. *Nature* **421**, 335–340 (2003).
45. Godfrey, S. J. & Currie, P. J. A in *Feathered Dragons: Studies on the Transition from Dinosaurs to Birds* (eds Currie, P. J. et al.) 144–149 (Indiana Univ. 2004).
46. Chiappe, L. M., Ji, S., Ji, Q. & Norell, M. A. *Anatomy and Systematics of the Confuciusornithidae (Theropoda: Aves) from the Late Mesozoic of Northeastern China* (American Museum of Natural History, 1999).
47. Martin, L. D., Zhou, Z., Hou, L. & Feduccia, A. *Confuciusornis sanctus* compared to *Archaeopteryx lithographica*. *Naturwissenschaften* **85**, 286–289 (1998).
48. O'Connor, J. K., Zheng, X., Xiaoli, W., Zhang, X. & Zhou, Z. The gastral basket in basal birds and their close relatives: size and possible function. *Vertebr. Palasiat.* **53**, 133–152 (2015).
49. Wang, M. & Zhou, Z. A morphological study of the first known piscivorous enantiornithine bird from the Early Cretaceous of China. *J. Vertebr. Paleontol.* **37**, e1278702 (2017).
50. Hou, L., Chiappe, L. M., Zhang, F. & Chuong, C. M. New Early Cretaceous fossil from China documents a novel trophic specialization for Mesozoic birds. *Naturwissenschaften* **91**, 22–25 (2004).
51. Chiappe, L. M. & Calvo, J. O. *Neuquenornis volans*, a new late Cretaceous bird (Enantiornithes: Avisauridae) from Patagonia, Argentina. *J. Vertebr. Paleontol.* **14**, 230–246 (1994).
52. Wang, Y. M., O'Connor, J. K., Li, D. Q. & You, H. L. New information on postcranial skeleton of the Early Cretaceous *Gansus yumenensis* (Aves: Ornithuromorpha). *Hist. Biol.* **28**, 666–679 (2016).
53. Zhou, S., Zhou, Z. & O'Connor, J. A new piscivorous ornithuromorph from the Jehol Biota. *Hist. Biol.* **26**, 608–618 (2014).
54. Wang, M., Zhou, Z. & Zhou, S. A new basal ornithuromorph bird (Aves: Ornithothoraces) from the Early Cretaceous of China with implication for morphology of early Ornithuromorpha. *Zool. J. Linn. Soc.* **176**, 207–223 (2016).
55. Wang, M., Zhou, Z. & Zhou, S. Corrigendum: Renaming of Bellulia Wang, Zhou & Zhou, 2016. *Zool. J. Linn. Soc.* **177**, 695 (2016).
56. O'Connor, J. K., Wang, M., Zhou, S. & Zhou, Z. Osteohistology of the Lower Cretaceous Yixian formation ornithuromorph (Aves) *Iteravis huchzermeyeri*. *Palaeontol. Electron.* **18.2.35A**, 1–11 (2015).
57. Lewis, P. O. A likelihood approach to estimating phylogeny from discrete morphological character data. *Syst. Biol.* **50**, 913–925 (2001).
58. Bell, A. & Chiappe, L. M. The Hesperornithiformes: a review of the diversity, distribution, and ecology of the earliest diving birds. *Diversity* **14**, 267 (2022).
59. Orkney, A., Bjarnason, A., Tronrud, B. C. & Benson, R. B. J. Patterns of skeletal integration in birds reveal that adaptation of element shapes enables coordinated evolution between anatomical modules. *Nat. Ecol. Evol.* **5**, 1250–1258 (2021).
60. Zhang, Y.-G., Li, Z., Liu, D., Liu, Q.-G. & Fu, L. The diversity of morphology of the avian sternum and its relationship with flight ability. *Sichuan J. Zool.* **5**, 677–686 (2011).
61. Yu, Y., Zhang, C. & Xu, X. Deep time diversity and the early radiations of birds. *Proc. Natl Acad. Sci. USA* **118**, e2019865118 (2021).
62. Wang, M., Lloyd, G. T., Zhang, C., Zhou, Z. & Lloyd, G. T. The patterns and modes of the evolution of disparity in Mesozoic birds. *Proc. R. Soc. B* **288**, 20203105 (2021).
63. Allen, V., Bates, K. T., Li, Z. & Hutchinson, J. R. Linking the evolution of body shape and locomotor biomechanics in bird-line archosaurs. *Nature* **497**, 104–107 (2013).
64. Macaulay, S. et al. Decoupling body shape and mass distribution in birds and their dinosaurian ancestors. *Nat. Commun.* **14**, 1575 (2023).
65. Olson, S. & Feduccia, A. Flight capability and the pectoral girdle of Archaeopteryx. *Nature* **278**, 247–248 (1979).
66. Chamberlain, F. W. *Atlas of Avian Anatomy: Osteology-Arthrology-Myology* (Michigan State College Agricultural Experiment Station, 1943).
67. Baumel, J. J. & Witmer, L. M. in *Handbook of Avian Anatomy: Nomina Anatomica Avium* (eds Baumel, J. J. et al.) 45–131 (Nuttall Ornithological Club, 1993).
68. Bock, W. J. The furcula and the evolution of avian flight. *Paleontol. J.* **47**, 1236–1244 (2013).
69. Meyers, R. A. & Stakebake, E. F. Anatomy and histochemistry of spread-wing posture in birds. 3. Immunohistochemistry of flight muscles and the 'shoulder lock' in albatrosses. *J. Morphol.* **263**, 12–29 (2005).
70. Pennycuick, C. J. *Animal Flight* (Edward Arnold, 1972).
71. Zhou, Z. & Farlow, J. O. in *New Perspectives on the Origin and Early Evolution of Birds: Proceedings of the International Symposium in Honor of* John H. *Ostrom* (eds Gauthier, J. & Gall, L. F.) 237–254 (Peabody Museum of Natural History Yale Univ., 2001).
72. Rayner, J. M. V. in *New Perspectives on the Origin and Early Evolution of Birds: Proceedings of the International Symposium in Honor of John H. Ostrom* (eds Gauthier, J. A. & Gall, L. F.) 363–388 (Peabody Museum of Natural History Yale Univ., 2001).
73. Sy, M. Funktionell-anatomische Untersuchungen am Vogelflügel. *J. Ornithol.* **84**, 199–296 (1936).
74. Brown, R. H. J. The flight of birds. *Biol. Rev.* **38**, 460–489 (1963).
75. Pennycuick, C. J. *Modelling the Flying Bird* (Elsevier, 2008).
76. Chiappe, L. M. & Walker, C. A. in *Mesozoic Birds: Above the Heads of Dinosaurs* (eds Chiappe, L. M. & Witmer, L. M.) 240–267 (Univ. California Press, 2002).
77. Wong, M. & Carter, D. Mechanical stress and morphogenetic endochondral ossification of the sternum. *J. Bone Joint Surg. Am.* **70**, 992–1000 (1988).
78. Falk, A. R., Kaye, T. G., Zhou, Z. & Burnham, D. A. Laser fluorescence illuminates the soft tissue and life habits of the early Cretaceous bird *Confuciusornis*. *PLoS ONE* **11**, e0167284 (2016).
79. Feduccia, A. *The Age of Birds* (Harvard Univ. Press, 1980).
80. Burnham, D. A., Feduccia, A., Martin, L. D. & Falk, A. R. Tree climbing—a fundamental avian adaptation. *J. Syst. Palaeontol.* **9**, 103–107 (2011).
81. Jasinoski, S. C., Russell, A. P. & Currie, P. J. An integrative phylogenetic and extrapolatory approach to the reconstruction of dromaeosaur (Theropoda: Eumaniraptora) shoulder musculature. *Zool. J. Linn. Soc.* **146**, 301–344 (2006).
82. Walker, C. A. & Dyke, G. J. Euenantiornithine birds from the Late Cretaceous of El Brete (Argentina). *Ir. J. Earth Sci.* **27**, 15–62 (2009).
83. Atterholt, J., Howard Hutchison, J. & O'Connor, J. K. The most complete enantiornithine from North America and a phylogenetic analysis of the Avisauridae. *PeerJ* **2018**, e5910 (2018).
84. Happ, J., Elsler, A., Kriwet, J., Pfaff, C. & Bochenski, Z. M. Two passeriform birds (Aves: Passeriformes) from the Middle Miocene of Austria. *PalZ* **96**, 313–321 (2022).
85. Chiappe, L. M., Serrano, F. J., Abramowicz, S. & Göhlich, U. B. Flight performance of the Early Cretaceous bird *Confuciusornis sanctus*: evidence from an exceptionally preserved fossil. *Span. J. Palaeontol.* **38**, 101–122 (2023).
86. Xu, X. et al. A new feathered maniraptoran dinosaur fossil that fills a morphological gap in avian origin. *Chin. Sci. Bull.* **54**, 430–435 (2009).

87. Gao, C. et al. A subadult specimen of the early Cretaceous bird *Sapeornis chaoyangensis* and a taxonomic reassessment of sapeornithids. *J. Vertebr. Paleontol.* **32**, 1103–1112 (2012).
88. Kundrát, M., Nudds, J., Kear, B. P., Lü, J. & Ahlberg, P. The first specimen of Archaeopteryx from the Upper Jurassic Mörnsheim Formation of Germany. *Hist. Biol.* **31**, 3–63 (2019).
89. Longrich, N. R., Vinther, J., Meng, Q., Li, Q. & Russell, A. P. Primitive wing feather arrangement in *Archaeopteryx lithographica* and *Anchiornis huxleyi*. *Curr. Biol.* **22**, 2262–2267 (2012).
90. Lambertz, M. & Perry, S. F. Remarks on the evolution of the avian sternum, dinosaur gastralia, and their functional significance for the respiratory apparatus. *Zool. Anz.* **255**, 80–84 (2015).
91. Xu, X. et al. An integrative approach to understanding bird origins. *Science* **346**, 1253293 (2014).
92. Wang, Y. M., O'Connor, J. K., Li, D. Q. & You, H. L. Previously unrecognized ornithuromorph bird diversity in the Early Cretaceous Changma Basin, Gansu Province, Northwestern China. *PLoS ONE* **8**, e77693 (2013).
93. Vazquez, R. J. The automating skeletal and muscular mechanisms of the avian wing (Aves). *Zoomorphology* **114**, 59–71 (1994).
94. Clarke, J. A., Zhou, Z. & Zhang, F. Insight into the evolution of avian flight from a new clade of Early Cretaceous ornithurines from China and the morphology of *Yixianornis grabaui*. *J. Anat.* **208**, 287–308 (2006).
95. Pittman, M. et al. Exceptional preservation and foot structure reveal ecological transitions and lifestyles of early theropod flyers. *Nat. Commun.* **13**, 7684 (2022).
96. Bell, A. & Chiappe, L. M. Statistical approach for inferring ecology of Mesozoic birds. *J. Syst. Palaeontol.* **9**, 119–133 (2011).
97. Brusatte, S. L., O'Connor, J. K. & Jarvis, E. D. The origin and diversification of birds. *Curr. Biol.* **25**, R888–R898 (2015).
98. Pei, R., Li, Q., Meng, Q., Norell, M. A. & Gao, K. Q. *New Specimens of* Anchiornis huxleyi *(Theropoda: Paraves) from the Late Jurassic of Northeastern China* (American Museum of Natural History, 2017).
99. Zhou, Z. & Zhang, F. Anatomy of the primitive bird *Sapeornis chaoyangensis* from the Early Cretaceous of Liaoning, China. *Can. J. Earth Sci.* **40**, 731–747 (2003).
100. Borchers, H. W. & Borchers, M. H. W. pracma. R package version 2.4.2. (2022).
101. Schneider, C. A., Rasband, W. S. & Eliceiri, K. W. NIH Image to ImageJ: 25 years of image analysis. *Nat. Methods* **9**, 671–675 (2012).
102. Anderson, J. F., Hall-Martin, A. & Russell, D. A. Long-bone circumference and weight in mammals, birds and dinosaurs. *J. Zool.* **207**, 53–61 (1985).
103. Christiansen, P. & Fariña, R. A. Mass prediction in theropod dinosaurs. *Hist. Biol.* **16**, 85–92 (2004).
104. Campbell, K. E. Jr & Marcus, L. in *Papers in Avian Paleontology Honoring Pierce Brodkorb* 395–412 (Natural History Museum of Los Angeles County, 1992).
105. Campione, N. E., Evans, D. C., Brown, C. M. & Carrano, M. T. Body mass estimation in non-avian bipeds using a theoretical conversion to quadruped stylopodial proportions. *Methods Ecol. Evol.* **5**, 913–923 (2014).
106. Campione, N. E. Extrapolating body masses in large terrestrial vertebrates. *Paleobiology* **43**, 693–699 (2017).
107. Campione, N. E. MASSTIMATE: body mass estimation equations for vertebrates. R package version 2.0 (2022).
108. Gingerich, P. D. Arithmetic or geometric normality of biological variation: an empirical test of theory. *J. Theor. Biol.* **204**, 201–221 (2000).
109. Cooney, C. R. et al. Mega-evolutionary dynamics of the adaptive radiation of birds. *Nature* **542**, 344–347 (2017).
110. Prum, R. O. et al. A comprehensive phylogeny of birds (Aves) using targeted next-generation DNA sequencing. *Nature* **526**, 569–573 (2015).
111. Jetz, W., Thomas, G. H., Joy, J. B., Hartmann, K. & Mooers, A. O. The global diversity of birds in space and time. *Nature* **491**, 444–448 (2012).
112. Bell, M. A. & Lloyd, G. T. strap. R package version 1.6-0 (2022).
113. del Hoyo, J., Elliott, A., Sargatal, J., Christie, D. A. & de Juana, E. (eds) *Handbook of the Birds of the World Alive* (Lynx Edicions, 2014).
114. *Birds of the World* (Cornell Laboratory of Ornithology, 2022).
115. Grafen, A. The phylogenetic regression. *Philos. Trans. R. Soc. Lond. B* https://doi.org/10.1098/rstb.1989.0106 (1989).
116. Orme, D. et al. caper. R package version 1.0.1 (2018).
117. Akaike, H. A new look at the statistical model identification. *IEEE Trans. Autom. Contr.* **19**, 716–723 (1974).
118. Sugiura, N. Further analysis of the data by Akaike's information criterion and the finite corrections. *Commun. Stat. Theory Method.* **7**, 13–26 (1978).
119. Choiniere, J. N. et al. Evolution of vision and hearing modalities in theropod dinosaurs. *Science* **613**, 610–613 (2021).
120. Fabbri, M. et al. Subaqueous foraging among carnivorous dinosaurs. *Nature* **603**, 852–857 (2022).
121. Felsenstein, J. Phylogenies and the comparative method. *Am. Nat.* **125**, 1–15 (1985).
122. Goolsby, E. W. Rapid maximum likelihood ancestral state reconstruction of continuous characters: a rerooting-free algorithm. *Ecol. Evol.* **7**, 2791–2797 (2017).
123. Revell, L. J. & Harmon, L. J. *Phylogenetic Comparative Methods in R* (Princeton Univ. Press, 2022).
124. Revell, L. J. phytools. R package version 1.5-1 (2023).
125. Bollback, J. P. SIMMAP: stochastic character mapping of discrete traits on phylogenies. *BMC Bioinf.* **7**, 88 (2006).
126. Revell, L. J. phytools: an R package for phylogenetic comparative biology (and other things). *Methods Ecol. Evol.* **3**, 217–223 (2012).
127. Motani, R. & Schmitz, L. Phylogenetic versus functional signals in the evolution of form–function relationships in terrestrial vision. *Evolution* **65**, 2245–2257 (2011).
128. Schmitz, L. & Motani, R. Nocturnality in dinosaurs inferred from scleral ring and orbit morphology. *Science* **332**, 705–708 (2011).
129. Hermanson, G. et al. Cranial ecomorphology of turtles and neck retraction as a possible trigger of ecological diversification. *Evolution* **76**, 2566–2586 (2022).
130. Navalón, G., Bjarnason, A., Griffiths, E. & Benson, R. B. J. Environmental signal in the evolutionary diversification of bird skeletons. *Nature* **611**, 306–311 (2022).
131. Watanabe, J. Quantitative discrimination of flightlessness in fossil Anatidae from skeletal proportions. *Auk* **134**, 672–695 (2017).
132. Stoessel, A., Kilbourne, B. M. & Fischer, M. S. Morphological integration versus ecological plasticity in the avian pelvic limb skeleton. *J. Morphol.* **274**, 483–495 (2013).
133. Mosimann, J. E. Size allometry: size and shape variables with characterizations of the lognormal and generalized gamma distributions. *J. Am. Stat. Assoc.* **65**, 930–945 (1970).
134. Adams, D. C. A method for assessing phylogenetic least squares models for shape and other high-dimensional multivariate data. *Evolution* **68**, 2675–2688 (2014).
135. Lowi-Merri, T. M. et al. Data from: Enlargement of sternum traits facilitated the evolution of powered flight in birds. *Dryad* https://doi.org/10.5061/dryad.jsxksn0ng (2025).

Acknowledgements

We would like to thank A. Bailleul, M. Wang and Z. Zhonghe at the Institute of Vertebrate Palaeontology and Palaeoanthropology, as well as H. Gibbins, C. Coy and P. Currie at the University of Alberta Laboratory for Vertebrate Palaeontology for assistance and access to fossil specimens. J. Benito and D. Field (University of Cambridge) provided the reconstruction of *Ichthyornis* used in this study. Useful

discussions, guidance and methodological assistance were provided by G. Funston, L. Mahler, J. Weir, D. McLennan and H. Larsson. This work was supported by a Natural Sciences and Engineering Research Council of Canada (NSERC) postgraduate scholarship (PGSD3-547147-2020) to T.M.L.-M., as well as NSERC Discovery Grants to D.C.E. (RGPIN-2018-06788) and S.C. (RGPIN-2018-06747). R.B. acknowledges support from the European Union's Horizon 2020 research and innovation programme 2014–2018 under grant agreement no. 677774 (European Research Council starting grant: TEMPO). The funders had no role in study design, data collection and analysis, decision to publish or preparation of the manuscript.

Author contributions

T.M.L.-M., R.B., S.C. and D.C.E. conceived and designed the project. R.B., H.H. and J.O. provided substantial data and verified data quality. T.M.L.-M. collected morphological and stratigraphic data, conducted all analyses and interpretations and wrote the initial paper draft. T.M.L.-M., R.B., H.H., J.O., S.C. and D.C.E. edited the paper.

Competing interests

The authors declare no competing interests.

Additional information

Extended data is available for this paper at https://doi.org/10.1038/s41559-025-02795-4.

Supplementary information The online version contains supplementary material available at https://doi.org/10.1038/s41559-025-02795-4.

Correspondence and requests for materials should be addressed to Talia M. Lowi-Merri.

Peer review information *Nature Ecology & Evolution* thanks Michael Pittman and the other, anonymous, reviewer(s) for their contribution to the peer review of this work.

https://doi.org/10.1038/s41559-025-02795-4

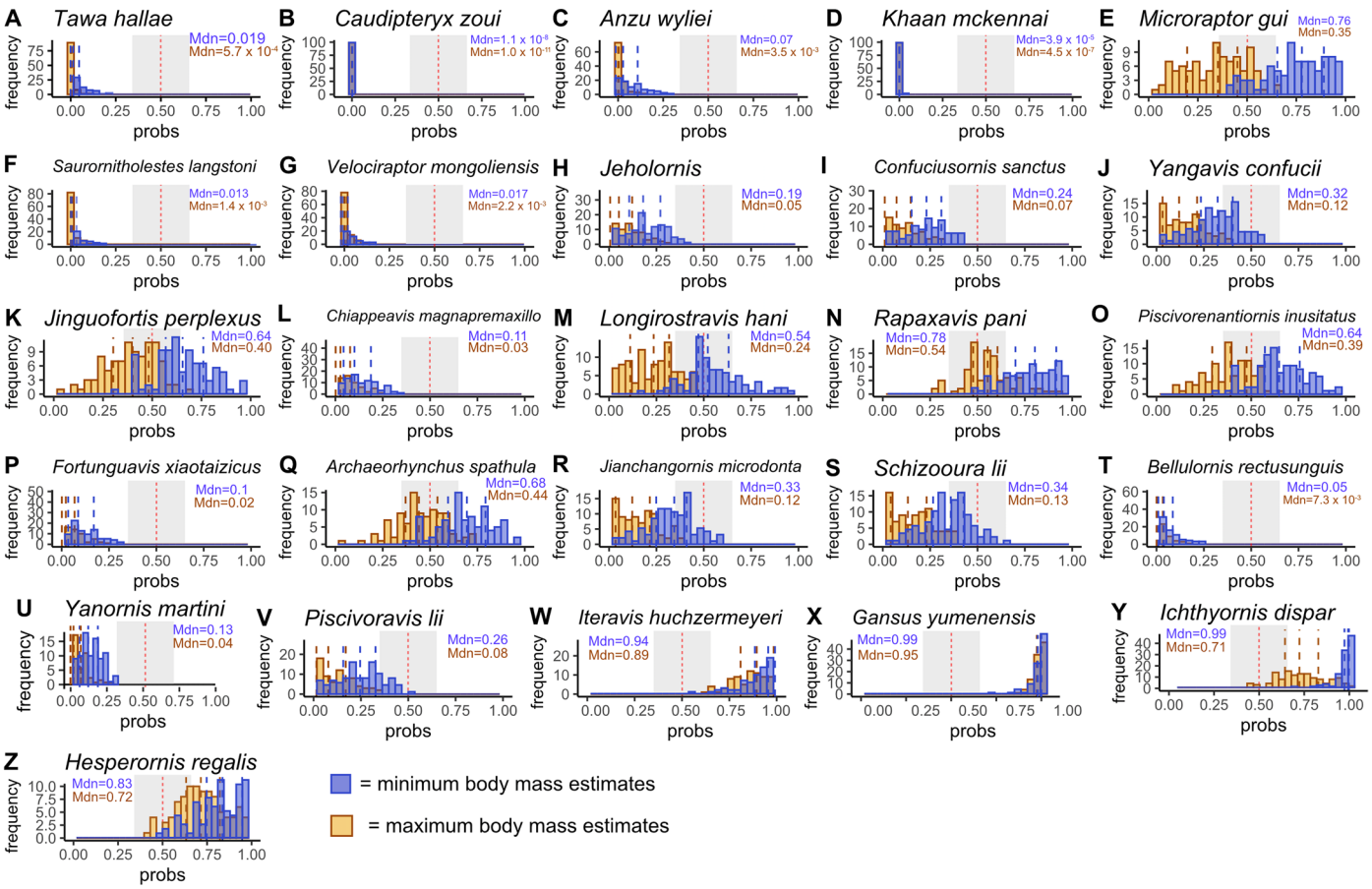

Extended Data Fig. 1 | Discriminant analysis results. Results from 100 iterations of the phylogenetic flexible discriminant analysis (pFDA) for the presence of forelimb propulsion ability in each of the fossil species, based on relative footprint area to body mass ($N = 112$ extant taxa; $N = 28$ fossil taxa). Blue values are from the pFDA that incorporates minimum body mass estimates, and orange values are maximum body mass estimates; corresponding dotted lines represent first quartile, median, and third quartile of estimates over 100 replicates of the analysis. X-axes represent probabilities for the presence of forelimb propulsion over 100 iterations of the analysis, and y-axes represent frequency of probabilities across 100 iterations. The red dotted line in the middle represents the 50% probability for flight presence, and the grey rectangle demarcates 0.33 to 0.67 probability, or the zone of uncertainty. Median probabilities ('Mdn') for flight presence are given for both body mass estimates. Values that are greater than 0.67 indicate that flight is likely present in the taxon, while less than 0.33 indicates that flight is likely absent; median probabilities in between fall in the uncertainty zone. Panels A-Z correspond with analyses performed for each fossil taxon.

https://doi.org/10.1038/s41559-025-02795-4

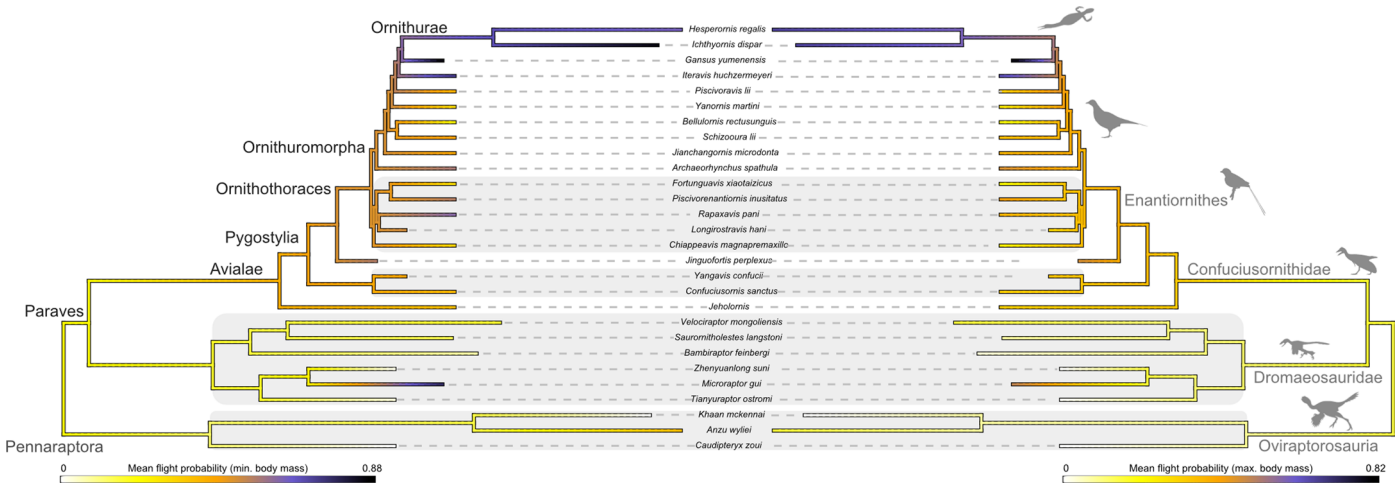

Extended Data Fig. 2 | Ancestral character estimation from results of discriminant analysis. Ancestral character estimation of median probability of flight presence across the dinosaur-bird transition from the discriminant analysis based on relative sternum plate area using minimum body mass estimates (left) and maximum body mass estimates (right) ($N = 28$ fossil taxa). Darker colours indicate a likely presence of flight ability in the taxon, lighter colours indicate likely absence of flight ability. The extant portion of the tree was condensed into a single branch labelled 'Neornithes', setting the tip value at 0, which represents the relative value for the ancestor of the living bird crown group, Neornithes.

nature portfolio

Corresponding author(s): Dr Talia Lowi-Merri

Last updated by author(s): Jun 2, 2025

Reporting Summary

Nature Portfolio wishes to improve the reproducibility of the work that we publish. This form provides structure for consistency and transparency in reporting. For further information on Nature Portfolio policies, see our Editorial Policies and the Editorial Policy Checklist.

Statistics

For all statistical analyses, confirm that the following items are present in the figure legend, table legend, main text, or Methods section.

n/a	Confirmed	
☐	☒	The exact sample size (*n*) for each experimental group/condition, given as a discrete number and unit of measurement
☐	☒	A statement on whether measurements were taken from distinct samples or whether the same sample was measured repeatedly
☐	☒	The statistical test(s) used AND whether they are one- or two-sided *Only common tests should be described solely by name; describe more complex techniques in the Methods section.*
☐	☒	A description of all covariates tested
☐	☒	A description of any assumptions or corrections, such as tests of normality and adjustment for multiple comparisons
☐	☒	A full description of the statistical parameters including central tendency (e.g. means) or other basic estimates (e.g. regression coefficient) AND variation (e.g. standard deviation) or associated estimates of uncertainty (e.g. confidence intervals)
☐	☒	For null hypothesis testing, the test statistic (e.g. *F*, *t*, *r*) with confidence intervals, effect sizes, degrees of freedom and *P* value noted *Give P values as exact values whenever suitable.*
☒	☐	For Bayesian analysis, information on the choice of priors and Markov chain Monte Carlo settings
☒	☐	For hierarchical and complex designs, identification of the appropriate level for tests and full reporting of outcomes
☒	☐	Estimates of effect sizes (e.g. Cohen's *d*, Pearson's *r*), indicating how they were calculated

Our web collection on statistics for biologists contains articles on many of the points above.

Software and code

Policy information about availability of computer code

Data collection	Custom R code was used when applicable, provided with submission and uploaded to Dryad repository
Data analysis	Custom R code was used and provided with submission and uploaded to Dryad repository

For manuscripts utilizing custom algorithms or software that are central to the research but not yet described in published literature, software must be made available to editors and reviewers. We strongly encourage code deposition in a community repository (e.g. GitHub). See the Nature Portfolio guidelines for submitting code & software for further information.

Data

Policy information about availability of data

All manuscripts must include a data availability statement. This statement should provide the following information, where applicable:

- Accession codes, unique identifiers, or web links for publicly available datasets
- A description of any restrictions on data availability
- For clinical datasets or third party data, please ensure that the statement adheres to our policy

Data and code provided with submission. Will be made public upon acceptance

Research involving human participants, their data, or biological material

Policy information about studies with human participants or human data. See also policy information about sex, gender (identity/presentation), and sexual orientation and race, ethnicity and racism.

Reporting on sex and gender	*Use the terms sex (biological attribute) and gender (shaped by social and cultural circumstances) carefully in order to avoid confusing both terms. Indicate if findings apply to only one sex or gender; describe whether sex and gender were considered in study design; whether sex and/or gender was determined based on self-reporting or assigned and methods used.* *Provide in the source data disaggregated sex and gender data, where this information has been collected, and if consent has been obtained for sharing of individual-level data; provide overall numbers in this Reporting Summary. Please state if this information has not been collected.* *Report sex- and gender-based analyses where performed, justify reasons for lack of sex- and gender-based analysis.*
Reporting on race, ethnicity, or other socially relevant groupings	*Please specify the socially constructed or socially relevant categorization variable(s) used in your manuscript and explain why they were used. Please note that such variables should not be used as proxies for other socially constructed/relevant variables (for example, race or ethnicity should not be used as a proxy for socioeconomic status).* *Provide clear definitions of the relevant terms used, how they were provided (by the participants/respondents, the researchers, or third parties), and the method(s) used to classify people into the different categories (e.g. self-report, census or administrative data, social media data, etc.)* *Please provide details about how you controlled for confounding variables in your analyses.*
Population characteristics	*Describe the covariate-relevant population characteristics of the human research participants (e.g. age, genotypic information, past and current diagnosis and treatment categories). If you filled out the behavioural & social sciences study design questions and have nothing to add here, write "See above."*
Recruitment	*Describe how participants were recruited. Outline any potential self-selection bias or other biases that may be present and how these are likely to impact results.*
Ethics oversight	*Identify the organization(s) that approved the study protocol.*

Note that full information on the approval of the study protocol must also be provided in the manuscript.

Field-specific reporting

Please select the one below that is the best fit for your research. If you are not sure, read the appropriate sections before making your selection.

☐ Life sciences ☐ Behavioural & social sciences ☒ Ecological, evolutionary & environmental sciences

For a reference copy of the document with all sections, see nature.com/documents/nr-reporting-summary-flat.pdf

Ecological, evolutionary & environmental sciences study design

All studies must disclose on these points even when the disclosure is negative.

Study description	Morphometric analysis of bird sternum using phylogenetic comparative methods
Research sample	A broad sample of extant bird skeletal data (112 extant species across 62 avian families), and 28 fossil pennaraptoran dinosaur taxa
Sampling strategy	Extant sample includes representatives of major avian families with different locomotor abilities. Fossil sample includes all known taxa with well-preserved sterna.
Data collection	Corresponding author collected measurements using custom code in R
Timing and spatial scale	Data was collected between February 2023 - May 2023, with additional data added during revision
Data exclusions	N/A
Reproducibility	Code has been provided for reproducibility purposes
Randomization	Randomization used in discriminant analysis; 100 iterations ran with each newly randomized
Blinding	Not relevant to study; morphological measurements collected.

Did the study involve field work? ☐ Yes ☒ No

Reporting for specific materials, systems and methods

We require information from authors about some types of materials, experimental systems and methods used in many studies. Here, indicate whether each material, system or method listed is relevant to your study. If you are not sure if a list item applies to your research, read the appropriate section before selecting a response.

Materials & experimental systems

n/a	Involved in the study
☒	☐ Antibodies
☒	☐ Eukaryotic cell lines
☐	☒ Palaeontology and archaeology
☐	☒ Animals and other organisms
☒	☐ Clinical data
☒	☐ Dual use research of concern
☒	☐ Plants

Methods

n/a	Involved in the study
☒	☐ ChIP-seq
☒	☐ Flow cytometry
☒	☐ MRI-based neuroimaging

Palaeontology and Archaeology

Specimen provenance	Specimens were photographed with permission at the Institute of Vertebrate Paleontology & Paleoanthropology, University of Alberta Vertebrate Paleontology lab, or taken from published sources
Specimen deposition	N/A
Dating methods	N/A

☐ Tick this box to confirm that the raw and calibrated dates are available in the paper or in Supplementary Information.

Ethics oversight	No ethics approval required for museum specimens

Note that full information on the approval of the study protocol must also be provided in the manuscript.

Animals and other research organisms

Policy information about studies involving animals; ARRIVE guidelines recommended for reporting animal research, and Sex and Gender in Research

Laboratory animals	N/A
Wild animals	N/A
Reporting on sex	Sex was not considered in this study, as there is no known sexual dimorphism in locomotion
Field-collected samples	N/A
Ethics oversight	No ethics approval required for museum specimens

Note that full information on the approval of the study protocol must also be provided in the manuscript.

Plants

Seed stocks	N/A
Novel plant genotypes	N/A
Authentication	N/A